JOINT WMO TECHNICAL PROGRESS REPORT ON THE GLOBAL DATA PROCESSING AND FORECASTING SYSTEM AND NUMERICAL WEATHER PREDICTION RESEARCH ACTIVITIES FOR 2020

Japan Meteorological Agency

1. Summary of highlights

(1) Operational use of Metop-C AMSU-A and MHS radiance data in JMA's global NWP system on September 15 2020 (4.2.1.2 (1))

(2) Operational use of EARS-ASCAT data in JMA's global early-run NWP system in February 2020 (4.2.1.2 (2))

(3) Operational use of GOES-16 AMVs and ScatSat-1/OSCAT data in JMA's global NWP system in July 2020 (4.2.1.2 (3))

(4) Refinement of parametrized surface drag processes, land surface processes and surface albedo and stratocumulus on sea ice on March 24 2020 (4.2.2.2)

(5) Implementation of a two-tiered SST approach (using precomputed SST from the Seasonal EPS) for Global EPS in the tropics and subtropics for forecasts longer than 11 days (4.2.5)

(6) Implementation of a new framework for data assimilation (ASUCA-Var) in Meso-scale Analysis in March 2020 (4.3.1.1 (1))

(7) Operational use of surface-sensitive clear-sky radiance data in JMA's local NWP system on July 29 2020 (4.3.1.2 (1))

(8) Optimization of initial and lateral boundary perturbations in the Meso-scale Ensemble Prediction System (MEPS) in September 2020 (4.3.5.1)

(9) Implementation of the new MOVE/MRI.COM-JPN coastal ocean analysis/prediction system in October 2020 (4.5.2.1 (4))

(10) Implementation of the 2D-Var data assimilation system for aerosol (Aeolian dust) analysis in January 2020

(11) Implementation of a nested regional chemical transport model with a horizontal resolution of 5 km in March 2020

2. Equipment in use

On 5 June 2018, an upgraded version of the computer system used for numerical analysis/prediction and satellite data processing was installed at the Office of Computer Systems Operations in Kiyose (around 30 km northwest of JMA's Tokyo Headquarters) and at the Osaka Regional Headquarters. The Kiyose, Tokyo and Osaka locations are connected via a wide-area network. The computer types

used in the system are listed in Table 2-1, and further details are provided in JMA (2019).

Table 2-1 System computer types

Supercomputers (Kiyose)　Cray XC50

Subsystems	2
Nodes per subsystem	2,816 computational 40 I/O
Processors	2 sockets for Intel Xeon Platinum 8160 processors per computational node 1 Intel Xeon E5-2699v4 processor per I/O node
Performance	9.08 PFlops per subsystem (3225.6 GFLOPS per node)
Main memory	264 TiB per subsystem (96 GiB per node)
High-speed storage*	DDN ExaScaler Lustre file system (4.8 PiB per subsystem)
Data transfer rate	14 GB/s (one way) (between any two nodes)
Operating system	Cray Linux Environment 6.0/SUSE 12.2

* Dedicated storage for supercomputers

Satellite Data Reception Servers (Kiyose) Server: HPE ProLiant DL360 Gen9

Servers	5
Processors	2 sockets for Intel Xeon E5-2620v3 processors
Main memory	64 GiB per server
Operating system	Red Hat Enterprise Linux Server 7.3

Satellite Imagery Processing Producing Servers (Kiyose): HPE ProLiant DL580 Gen9

Servers	8
Processors	4 sockets for Intel Xeon E7-8880v3 processors
Main memory	256 GiB per server
Operating system	Red Hat Enterprise Linux Server 7.3

Satellite Product Servers (Kiyose): HPE ProLiant DL380 Gen9

Servers	10
Processors	2 sockets for Intel Xeon E5-2670v3 processors
Main memory	192 GiB per server
Operating system	Red Hat Enterprise Linux Server 7.3

Operation Control Servers (Kiyose): Hitachi HA8000 RS210AN1

Servers	8
Processors	2 sockets for Intel Xeon E5-2640v3 processors
Main memory	32 GiB per server
Operating system	Red Hat Enterprise Linux Server 7.3

Division Task Processing Servers (Kiyose): HPE ProLiant DL580 Gen9

Servers	12
Processors	4 sockets for Intel Xeon E7-8880v3 processors
Main memory	128 GiB per server
Operating system	Red Hat Enterprise Linux Server 7.3

Decoding Servers (Kiyose): HPE ProLiant DL580 Gen9

Servers	2
Processors	4 sockets for Intel Xeon E7-8860v3 processors
Main memory	256 GiB per server
Operating system	Red Hat Enterprise Linux Server 7.3

NWP BCP Servers (Osaka): HPE ProLiant DL360 Gen9

Servers	2
Processors	2 sockets for Intel Xeon E5-2680v3 processors
Main memory	256 GiB per server
Operating system	Red Hat Enterprise Linux Server 7.3

Satellite Data Reception Servers (Osaka): HPE ProLiant DL360 Gen9

Servers	2
Processors	2 sockets for Intel Xeon E5-2620v3 processors
Main memory	64 GiB per server
Operating system	Red Hat Enterprise Linux Server 7.3

Satellite Imagery Processing Servers (Osaka): HPE ProLiant DL360 Gen9

Servers	4
Processors	2 sockets for Intel Xeon E5-2698v3 processors
Main memory	128 GiB per server
Operating system	Red Hat Enterprise Linux Server 7.3

External Storage System (Kiyose)

Shared storage**	Hitachi VSP G800 (6.06 PB total, RAID 6)
High-capacity storage (1) **	Hitachi VSP G800 (6.08 PB total, RAID 6)
High-capacity storage (2) **	Hitachi VSP G800 (3.04 PB total, RAID 6)
High-capacity storage (3) **	Hitachi VSP G800 (16.02 PB total, RAID 6)
Long-term Archival Storage	IBM TS4500 tape library (80 PB total)

** Shared by supercomputers and servers

Wide Area Network

Between HQ and Kiyose: Network bandwidth 1,200 Mbps (two independent 100-Mbps and 1-Gbps (best-effort) WANs)

Between Kiyose and Osaka: Network bandwidth 200 Mbps (two independent 100-Mbps WANs)

3. Data and Products from GTS and other sources in use

3.1 Observation

A summary of data received through the GTS and other sources and processed at JMA is given in Table 3.1-1.

Table 3.1-1 Number of observation reports in use

SYNOP/SHIP/SYNOP MOBIL	200,000/day
BUOY	58,000/day
TEMP/PILOT	7500/day
AIREP/AMDAR	1,100,000/day
PROFILER	8,000/day
AMSR2	14,000,000/day
GPM/GMI	10,200,000/day
Coriolis/WindSat	6,800,000/day
FY-3/MWRI	12,000,000/day
Aqua/AIRS, AMSU-A	270,000/day
NOAA/AMSU-A	960,000/day
Metop/AMSU-A	960,000/day
NOAA/MHS	5,800,000/day
Metop/MHS	8,700,000/day
Metop/IASI	600,000/day
Metop/ASCAT	8,000,000/day
ScatSat-1/OSCAT	1,200,000/day
Suomi-NPP/ATMS	3,000,000/day
Suomi-NPP/CrIS	3,000,000/day
NOAA/ATMS	3,000,000/day
NOAA/CrIS	3,000,000/day
Megha-Tropiques/SAPHIR	9,000,000/day
GOES/CSR	6,200,000/day
Himawari/CSR	1,300,000/day
METEOSAT/CSR	1,800,000/day
GNSS-RO	460,000/day
AMV	10,000,000/day
SSMIS	14,000,000/day
GNSS-PWV	4,200,000/day
AMeDAS	232,400/day
Radar Reflectivity	4,200/day
Radial Velocity	4,200/day

3.2 Forecast products

Grid Point Value (GPV) products of the global prediction model from ECMWF, NCEP, UKMO, BOM,

ECCC, DWD, KMA and CMA are used for internal reference and monitoring. The products of ECMWF are received via the GTS, and the other products are received via the Internet.

4. Forecasting systems

4.1 System run schedule and forecast ranges

Table 4.1-1 summarizes the system run schedule and forecast ranges.

Table 4.1-1 Schedule of the analysis and forecast system

Model	Initial time (UTC)	Run schedule (UTC)	Forecast range (hours)
Global Analysis/Forecast	00	0220 – 0335	132
	06	0820 – 0935	132
	12	1420 – 1605	264
	18	2020 – 2135	132
Meso-scale Analysis/Forecast	00	0055 – 0200	51
	03	0355 – 0500	39
	06	0655 – 0800	39
	09	0955 – 1100	39
	12	1255 – 1400	51
	15	1555 – 1700	39
	18	1855 – 2000	39
	21	2155 – 2300	39
Meso-scale Ensemble Forecast	00	0150 – 0320	39
	06	0750 – 0920	39
	12	1350 – 1520	39
	18	1950 – 2120	39
Local Analysis/Forecast	00, 01, 02, 03, 04, 05, 06, 07, 08, 09, 10, 11, 12, 13, 14, 15, 16, 17, 18, 19, 20, 21, 22, 23	0035 – 0125, 0135 – 0225, 0235 – 0325, 0335 – 0425, 0435 – 0525, 0535 – 0625, 0635 – 0725, 0735 – 0825, 0835 – 0925, 0935 – 1025, 1035 – 1125, 1135 – 1225, 1235 – 1325, 1335 – 1425, 1435 – 1525, 1535 – 1625, 1635 – 1725, 1735 – 1825, 1835 – 1925, 1935 – 2025, 2035 – 2125, 2135 – 2225, 2235 – 2325, 2335 – 0025	10
Ocean Wave Forecast	00	0330 – 0400	132
	06	0930 – 1000	132
	12	1530 – 1600, 1840–1900	264
	18	2130 – 2200	132
Wave Ensemble Forecast	00	0445 – 0545	264
	12	1900 – 2000	264
Storm Surge Forecast	00	0200 – 0255	39
	03	0500 – 0555	39
	06	0800 – 0855	39
	09	1100 – 1155	39
	12	1400 – 1455	39
	15	1700 – 1755	39
	18	2000 – 2055	39
	21	2300 – 2355	39
Asian-area Storm	00	0340 – 0350	72

Surge Forecast	06 12 18	0940 – 0950 1540 – 1550 2140 – 2150	72 72 72
Global Ensemble Forecast (Typhoon/One-week)	00 06 12 18	0305 – 0355 0905 – 0935 1505 – 1555 2105 – 2135	264 132 264 132
Global Ensemble Forecast (Two-week)	00 12	0530 – 0630 1730 – 1830	264 – 432 264 – 432
Global Ensemble Forecast (One-month)	00 12	0655 – 0755 1855 – 1955 (every Tuesday and Wednesday)	432 – 816 432 – 816
Seasonal Ensemble Forecasts	00	1730 – 1910 (every 5 days)	(7 months)

4.2 Medium-range forecasting system (4 – 10 days)

4.2.1 Data assimilation, objective analysis and initialization

4.2.1.1 In operation

(1) Global Analysis (GA)

Hybrid four-dimensional variational (4D-Var) data assimilation involving the use of a Local Ensemble Transform Kalman Filter (LETKF; Hunt et al., 2007) is employed in atmospheric analysis for the Global Spectral Model (GSM). Three-hour ensemble forecasting initialized with the LETKF is used in 4D-Var with the extended control variable method of Lorenc (2003) to create flow-dependent background error covariances, which are blended with climatological background error covariances. Analysis from 4D-Var is used to re-center LETKF ensemble analysis, and Figure 4.2.1.1 (1)-1 outlines the hybrid LETKF/4D-Var. An incremental method is adopted to improve computational efficiency using outer-loop iterations, with increments evaluated at a lower horizontal resolution (TL319). The increment is then interpolated and used to update the model trajectory at the original resolution (TL959), and the updated trajectory is used to refine the cost function for subsequent inner-loop iterations.

The Global Analysis (GA) is performed at 00, 06, 12 and 18 UTC. An early analysis with a short cut-off time is performed to prepare initial conditions for operational forecasting, and a cycle analysis with a long cut-off time is performed to maintain the quality of the global data assimilation system.

The specifications of the atmospheric analysis schemes are listed in Table 4.2.1.1 (1)-1 and 4.2.1.1 (1)-2.

The global land surface analysis system has been in operation since March 2000 to provide the initial conditions of land surface parameters for the GSM. The system includes daily global snow depth analysis, described in Table 4.2.1.1 (1)-3, to obtain appropriate initial conditions for snow coverage and depth.

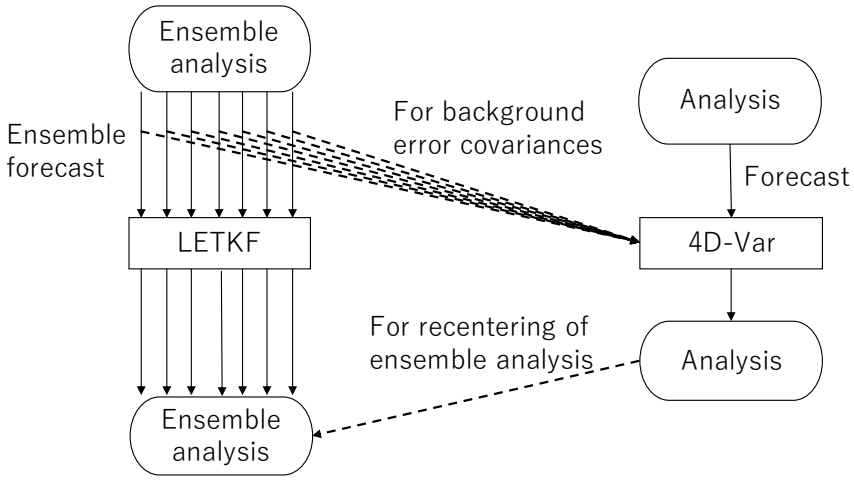

Figure 4.2.1.1 (1)-1. Hybrid LETKF/4D-Var

Table 4.2.1.1 (1)-1. Specifications of 4D-Var in GA

Analysis scheme	Incremental hybrid 4D-Var using LETKF
Data cut-off time	2 hours and 20 minutes for early run analysis at 00, 06, 12 and 18 UTC 11 hours and 50 minutes for cycle run analysis at 00 and 12 UTC 7 hours and 50 minutes for cycle run analysis at 06 and 18 UTC
First guess	6-hour forecast by the GSM
Domain configuration (Outer step)	Globe TL959, Reduced Gaussian grid, roughly equivalent to 0.1875˚ (20 km) [1920 (tropic) – 60 (polar)] x 960
(Inner step)	TL319, Reduced Gaussian grid, roughly equivalent to 0.5625˚ (55 km) [640 (tropic) – 60 (polar)] x 960
Vertical coordinates	σ-p hybrid
Vertical levels	100 forecast model levels up to 0.01 hPa + surface
Outer-loop iterations	2
Inner-loop iterations	Approx. 35
Control variables for climatological background error covariance	Relative vorticity, unbalanced divergence, unbalanced temperature, unbalanced surface pressure and natural logarithm of specific humidity
Covariance inflation for ensemble covariance	Adaptive multiplicative covariance inflation (as per LETKF application) Additional covariance inflation is applied to create vertical profiles for the horizontal global mean of standard deviation from ensemble covariances consistent with those from climatological background error covariances.
Localization for ensemble covariance	Gaussian function. The localization scale for which the localization function is $1/\sqrt{e}$ is set to 800 km in the horizontal domain and a 0.8-scale height in the vertical domain.
Weighting for hybrid covariance	0.85 for climatological covariance and 0.15 for ensemble covariance under 50 hPa. Values approach 1 and 0 above 50 hPa, respectively.
Analysis variables	Wind, surface pressure, specific humidity and temperature
Observations (as of 31 December 2020)	SYNOP, METAR, SHIP, BUOY, TEMP, PILOT, Wind Profiler, AIREP, AMDAR, Typhoon Bogus; atmospheric motion vectors (AMVs) from

	Himawari-8, GOES-16, Meteosat-8, 11; MODIS polar AMVs from Terra and Aqua satellites; AVHRR polar AMVs from NOAA and Metop satellites; LEO-GEO AMVs; ocean surface wind from Metop-A, B, C/ASCAT, ScatSat-1/OSCAT; radiances from NOAA-15, 18, 19/ATOVS, Metop-A, B, C/ATOVS, Aqua/AMSU-A, DMSP-F17, 18/SSMIS, Suomi-NPP, NOAA-20/ATMS, GCOM-W/AMSR2, GPM-core/GMI, Coriolis/WindSat, FY-3C/MWRI, Megha-Tropiques/SAPHIR, Aqua/AIRS, Metop-A,B/IASI, Suomi-NPP, NOAA-20/CrIS, clear sky radiances from the water vapor channels (WV-CSRs) of Himawari-8, GOES-15, 16, Meteosat-8, 11; GNSS RO bending angle data from Metop-A, B/GRAS, COSMIC/IGOR, TerraSAR-X/IGOR; zenith total delay data from ground-based GNSS
Assimilation window	6 hours

Table 4.2.1.1 (1)-2. Specifications of the LETKF in GA

Data cut-off time	As per 4D-Var
First guess	Own 6-hour forecast
Domain configuration	As per 4D-Var inner step
Vertical coordinates	As per 4D-Var
Vertical levels	As per 4D-Var
Ensemble size	50 members
Perturbations to model physics	Stochastic perturbation of physics tendency
Initialization	Horizontal divergence adjustment based on analysis of surface pressure tendency (Hamrud et al., 2015)
Covariance inflation	Adaptive multiplicative covariance inflation
Localization	Gaussian function. The localization scale for which the localization function is $1/\sqrt{e}$ is set to 400 km in the horizontal domain (300 km for humidity-sensitive observations), a 0.4 scale height in the vertical domain (0.8 for surface pressure and ground-based GNSS zenith total-delay observations) and three hours in the temporal domain. For satellite radiance observations, the maximum of the square of the weighting function divided by its peak value and the Gaussian function with a $0.4\sqrt{2}$ scale height centered at the peak of the weighting function is used as the vertical localization function.
Re-centering	Ensemble analysis is re-centered so that the ensemble mean is consistent with 4D-Var.
Analysis variables	As per 4D-Var
Observation	As per 4D-Var, but without the use of Aqua/AIRS, Metop-A, B/IASI and Suomi-NPP, and NOAA-20/CrIS data
Assimilation window	As per 4D-Var

Table 4.2.1.1 (1)-3. Specifications of snow depth analysis in GA

Methodology	Two-dimensional Optimal Interpolation scheme
Domain and grids	Global, $1^\circ \times 1^\circ$ equal latitude-longitude grids
First guess	Derived from previous snow depth analysis and USAF/ETAC Global Snow Depth climatology (Foster and Davy, 1988)
Data used	SYNOP snow depth data
Frequency	Daily

(2) Typhoon bogussing in GA

For typhoon forecasts over the western North Pacific, typhoon bogus data are generated to represent typhoon structures accurately in the initial field of forecast models. These data consist of information on artificial sea-surface pressure and wind data around a typhoon. The structure is axi-asymmetric. Symmetric bogus profiles are first generated automatically based on the central pressure and 30-kt

wind speed radius of typhoons. Asymmetric components are then retrieved from the first-guess fields and added to these profiles. Finally, the profiles are used as pseudo-observation data for GA.

4.2.1.2 Research performed in this field

(1) Operational use of Metop-C AMSU-A and MHS Radiance Data in JMA's Global NWP system

JMA began to assimilate data from the Advanced Microwave Sounding Unit-A (AMSU-A) and Microwave Humidity Sounder (MHS) onboard Metop-C in its global NWP system on September 15 2020. Quality control (QC) and error handling for the assimilation of Metop-C /AMSU-A and MHS radiance data (such as channel selection, thinning distance, observation errors, rain/cloud detection and bias correction (static scan bias correction and variational bias correction)) follow those implemented for other AMSU-A and MHS, as there are no significant differences in data quality. Currently, AMSU-A channels 4 – 14 and MHS channels 3 – 5 are assimilated. AMSU-A radiance data were assimilated under clear-sky conditions, and MHS radiance data were assimilated under all-sky conditions (Shimizu et al. 2020). Assimilation experiments with Metop-C /AMSU-A and MHS data showed that the additional information improved first-guess accuracy, which also infers improved analysis accuracy. The experiments also showed improved accuracy of forecast fields for geopotential height, temperature, humidity and wind speed.

(2) Operational use of EARS-ASCAT data in JMA's global early-run NWP system

EUMETSAT provides EARS-ASCAT (Regional Data Service of ASCAT products), which is available around 90 minutes earlier than global ASCAT wind data. Under EARS-ASCAT, observation data are collected and processed when Metop satellites pass over ground base stations in the North Atlantic Ocean and Europe. It is expected that the amount of ASCAT wind data used in JMA's global early analysis, which have a short cutoff time (2 hours and 20 minutes), is expected to increase, and the number of ASCAT wind data used in JMA's global early-run analysis increased by up to 10% from the use of EARS-ASCAT data. These data were adopted in global early-run analysis with the same quality control used for other ASCAT wind data on February 26 2020.

(3) Operational use of GOES-16 AMVs and ScatSat-1/OSCAT data in JMA's global NWP system

Observing-system experiments assimilating both GOES-16 AMVs and ScatSat-1/OSCAT data in the GSM were performed to verify effects on analysis and forecast fields. The first-guess field is modified to be more consistent with observation from humidity sounding channels, which are sensitive to upper air (e.g., ATMS Ch. 21 and 22), and temperature sounding channels sensitive to lower air (e.g., ATMS Ch. 6). The first-guess wind field for the troposphere changes neutrally or improves slightly to match radiosonde observation. The results suggest that the upper-troposphere circulation field and lower-air convergence/divergence positions in the first guess are improved by assimilation of GOES-16 AMVs and OSCAT wind data. Verification of effects on tropical cyclone track prediction in summer 2019 for the Atlantic and eastern Pacific regions shows that predicted position errors are reduced by assimilating GOES-16 AMVs and OSCAT wind data. GOES-16 AMVs and ScatSat-

1/OSCAT data began to be assimilated into JMA's global NWP system on July 29 2020.

(4) Ensemble member increase for flow-dependent background error covariances

Testing was performed with a greater number of ensemble members to create flow-dependent background error covariances in hybrid LETKF/4D-Var. The number of members was increased from 50 to 100 to reduce sampling errors, weighting for ensemble covariance was increased, and the horizontal/vertical localization function length scales in 4D-Var and LETKF were tuned. Retrospective experiments covering periods of at least a month in summer 2018 and winter 2018/19 showed increased ensemble spreads and reduced standard deviations of first-guess departures as compared to the current operational version. See Yokota et al. (2021) for more details. These upgrades are expected to be implemented in 2021.

(5) Improvement of surface analysis

Improved snow-depth analysis and soil-moisture analysis are expected to be implemented in 2021.

In the improved snow depth analysis, the first guess is replaced with forecast snow depth corrected using satellite-based snow area estimations. Harnessing with the first-guess replacement, correlation length and magnitude of background error are optimized to increase the contribution of the first guess to analysis. These improvements mitigate excessive spread of snow analysis data over observation-sparse areas and reduce systematic errors in shortwave radiative flux for snow-covered surfaces.

Soil moisture analysis assimilating screen-level temperature and relative humidity analysis with a simplified Extended Kalman Filter were also developed. The system initializes soil moisture from the surface to a depth of 0.19 m, thereby enabling representation of variations associated with daily weather conditions and reducing temperature errors for the lower troposphere.

4.2.2 Model

4.2.2.1 In operation

(1) Global Spectral Model (GSM)

The specifications of the operational Global Spectral Model (GSM2003; TL959L100) are summarized in Table 4.2.2.1 (1)-1.

The GSM forecasts with 00, 06 and 18 UTC initials were extended from 84 to 132 hours in June 2018 in association with the supercomputer system update. JMA runs the GSM four times a day at 00, 06 and 18 UTC with a forecast time of 132 hours and at 12 UTC with a forecast time of 264 hours.

Table 4.2.2.1 (1)-1 GSM 11-day forecast specifications

1. System	
Model (version)	Global Spectral Model (GSM2003)
Date of implementation	24 March 2020
2. Configuration	
Horizontal resolution (Grid spacing)	Spectral triangular 959 (TL959), reduced Gaussian grid system, roughly equivalent to 0.1875 × 0.1875° (20 km) in latitude and longitude
Vertical resolution (model top)	100 stretched sigma pressure hybrid levels (0.01 hPa)
Forecast length (initial time)	132 hours (00, 06, 18 UTC) 264 hours (12 UTC)
Coupling to ocean/wave/sea ice models	None
Integration time step	400 seconds
3. Initial conditions	
Data assimilation	Four-dimensional variational (4D-Var) method
4. Surface boundary conditions	
Treatment of sea surface	Climatological sea surface temperature with daily analysis anomaly Climatological sea ice concentration with daily analysis anomaly
Land surface analysis	Snow depth: two-dimensional optimal interpolation scheme Temperature: first guess Soil moisture: climatology
5. Other details	
Land surface and soil	Simple Biosphere (SiB) model
Radiation	Two-stream with delta-Eddington approximation for short wave (hourly) Two-stream absorption approximation method for long wave (hourly)
Numerical techniques	Spectral (spherical harmonic basis functions) in horizontal, finite differences in vertical Two-time-level, semi-Lagrangian, semi-implicit time integration scheme Hydrostatic approximation
Planetary boundary layer	Mellor and Yamada level-2 turbulence closure scheme Similarity theory in bulk formulae for surface layer
Convection	Prognostic Arakawa-Schubert cumulus parameterization
Cloud	PDF-based cloud parameterization
Subgrid orography	Low-level blocked-flow drag, gravity wave drag and turbulent orographic-form drag schemes
Non-orographic gravity wave drag	Spectral gravity wave forcing scheme
6. Further information	
Operational contact point	globalnwp@met.kishou.go.jp
System documentation URL	https://www.jma.go.jp/jma/jma-eng/jma-center/nwp/nwp-top.htm

4.2.2.2 Research performed in this field

(1) Upgrade of the GSM

JMA upgraded its Global Spectral Model (GSM) in March 24 2020 to refine parametrized surface drag processes, land surface processes, and surface albedo and stratocumulus on sea ice. Introduction of low-level blocked-flow drag, gravity wave drag and turbulent orographic-form drag schemes significantly reduced forecast errors around synoptic-scale troughs and ridges in the lower

and middle troposphere over Eurasia. Updating of diagnostic schemes for the fraction of snow coverage and soil thermal conductivity in the land surface model reduced systematic errors in surface variables. A new sea ice albedo scheme and inactivation of the marine stratocumulus scheme on sea ice also reduced errors in radiative surface shortwave fluxes.

JMA plans to upgrade the GSM in 2021 with vertical resolution enhanced from 100 to 128 levels to reduce discretization errors in the dynamical process and improve atmospheric representation.

4.2.3 Operationally available NWP products

The model output products shown below from the GSM are disseminated through JMA's radio facsimile broadcast (JMH) service, GTS and the Global Information System Centre (GISC) Tokyo website.

Table 4.2.3-1 List of facsimile charts transmitted via the GTS and JMH

The contour lines (upper-case letters) are: D: dew-point depression (T - T_d); E: precipitation; H: geopotential height; J: wave height; O: vertical velocity (ω); P: sea level pressure; T: temperature; W: isotach wind speed; Z: vorticity; δ: anomaly from climatology; μ: average over time. The other symbols are: a: wind arrows; b: observation plots; d: hatch for dewpoint depression < 3 K; g: arrows for prevailing wave direction; j: jet axis; m: wave period in digits; t: temperature in digits; x: streamlines. The subscripts in the table indicate: $_{srf}$: surface; $_{trp}$: tropopause; digit (ex. $_{500}$) pressure in hPa. The superscripts indicate dissemination channels and time: ^{G}: sent to GTS; ^{J}: sent to JMH; ^{12}: for 12 UTC only; ^{5}: statistics for pentad sent once per five days for 00 UTC; ^{m}: statistics for the month sent monthly for 00 UTC.

Model	Area		Forecast Time [h]						
		Analysis	12	24	36	48	72	96 120	144 168 192
GSM	Asia	$HWbt_{300}^{G}$ $HTbt_{500}^{GJ}$ $HTbd_{700}^{G}$ $HTbd_{850}^{GJ}$		EP_{srf}^{G}		HZ_{500}^{G} $Ta_{850}O_{700}^{G12}$ EP_{srf}^{GJ}		EP_{srf}^{GJ12} HZ_{500}^{G12} $P_{srf}T_{850}^{G12}$	
	East Asia	HZ_{500}^{G} $Ta_{850}O_{700}^{G}$		HZ_{500}^{GJ} $Dd_{700}T_{500}^{GJ}$ $Ta_{850}O_{700}^{GJ}$ EPa_{srf}^{GJ}					
	Asia-Pacific	$HWajt_{200}H_{trp}^{G}$ $HWat_{250}^{G}$		$HTWa_{250}^{G}$ $HTWa_{500}^{G}$					
	NW Pacific	x_{200}^{G} x_{850}^{G}		x_{200}^{G} x_{850}^{G}		x_{200}^{G} x_{850}^{G}			
	N Hem.	HT_{500}^{G12}							
Ocean Wave	Japan	$Jabgm_{srf}^{GJ}$							
	NW Pacific	$Jbgm_{srf}^{GJ}$		Jgm_{srf}^{J}		Jgm_{srf}^{J}			

Table 4.2.3-2 List of GPV products (GRIB2) distributed via the GISC Website

Symbols: H: geopotential height; U: eastward wind; V: northward wind; W: wind speed; G: gusts; T: temperature; R: relative humidity; O: vertical velocity (ω); Z: vorticity; X: stream function; Y: velocity potential; Di: relative divergence; P: pressure; Ps: sea level pressure; E: rainfall; N: total cloud cover; Ch: high cloud cover; Cm: middle cloud cover; Cl: low cloud cover. The prefixes μ and σ represent the average and standard deviations of ensemble prediction results, respectively. The prefix ρ represents the probability of ensemble prediction results, and parentheses represent probability thresholds.

Model	GSM	GSM
Area and resolution	Whole globe, Region II 0.25° × 0.25° (surface), 0.5° × 0.5° (surface, isobar level)	Whole globe, Region II 1.25° × 1.25°
Elements	10 hPa: H, U, V, T, R, O 20 hPa: H, U, V, T, R, O 30 hPa: H, U, V, T, R, O 50 hPa: H, U, V, T, R, O 70 hPa: H, U, V, T, R, O 100 hPa: H, U, V, T, R, O 150 hPa: H, U, V, T, R, O 200 hPa: H, U, V, T, R, O, X, Y 250 hPa: H, U, V, T, R, O 300 hPa: H, U, V, T, R, O 400 hPa: H, U, V, T, R, O 500 hPa: H, U, V, T, R, O, Z 600 hPa: H, U, V, T, R, O 700 hPa: H, U, V, T, R, O 800 hPa: H, U, V, T, R, O 850 hPa: H, U, V, T, R, O, X, Y 900 hPa: H, U, V, T, R, O 925 hPa: H, U, V, T, R, O 950 hPa: H, U, V, T, R, O 975 hPa: H, U, V, T, R, O 1,000 hPa: H, U, V, T, R, O Surface: U, V, T, R, P, Ps, E, N, Ch, Cm, Cl	10 hPa: H, U, V, T 20 hPa: H, U, V, T 30 hPa: H, U, V, T 50 hPa: H, U, V, T 70 hPa: H, U, V, T 100 hPa: H, U, V, T 150 hPa: H, U, V, T 200 hPa: H, U, V, T, X, Y 250 hPa: H, U, V, T, Z, Di 300 hPa: H, U, V, T, R, O 400 hPa: H, U, V, T, R, O 500 hPa: H, U, V, T, R, O, Z 600 hPa: H, U, V, T, R, O 700 hPa: H, U, V, T, R, O, Z, Di 850 hPa: H, U, V, T, R, O, X, Y 925 hPa: H, U, V, T, R, O, Z, Di 1,000 hPa: H, U, V, T, R, O Surface: U, V, T, R, Ps, E
Forecast hours	0 – 132 every 3 hours, 138 – 264 every 6 hours (12 UTC)	0 – 132 every 6 hours, 144 – 264 every 12 hours (12 UTC)
Initial times	00, 06, 12, 18 UTC	00, 06, 12, 18 UTC

Model	Global Ensemble Forecast (One-week)
Area and resolution	Whole globe 1.25° × 1.25°
Levels and elements	250 hPa: μU, μV, σU, σV 500 hPa: μH, σH 850 hPa: μU, μV, σU, σV, μT, σT, μW, σW, ρT (±1, ±1.5, ±2 standard deviation with respect to reanalysis climatology) 1,000 hPa: μH, σH Surface: μP, σP, ρE (1, 5, 10, 25, 50, 100 mm/24hours), ρW (10, 15, 25 m/s), ρG (10, 15, 25 m/s),
Forecast hours	0 – 264 every 12 hours
Initial times	00 UTC and 12 UTC

Table 4.2.3-3 List of GPV products (GRIB) distributed via the GISC website and the GTS

Symbols: D: dew-point depression; E: precipitation; G: prevailing wave direction; H: geopotential height; J: wave height; M: wave period; O: vertical velocity (ω); P: sea level pressure; R: relative humidity; T: temperature; U: eastward wind; V: northward wind; X: stream function; Y: velocity potential; Z: vorticity;
The prefixes μ and σ represent the average and standard deviations of ensemble prediction results, respectively. The symbols °, *, ¶, §, ‡ and † indicate limitations on forecast hours or initial times as shown in the notes below.

Model	GSM	GSM	GSM
Destination	GTS, GISC	GTS, GISC	GTS, GISC
Area and resolution	Whole globe, 1.25° × 1.25°	20°S – 60°N, 60°E – 160°W 1.25° × 1.25°	Whole globe, 2.5° × 2.5°
Levels and elements	10 hPa: H, U, V, T 20 hPa: H, U, V, T 30 hPa: H, U, V, T 50 hPa: H, U, V, T 70 hPa: H, U, V, T 100 hPa: H, U, V, T 150 hPa: H, U, V, T 200 hPa: H, U, V, T, X, Y 250 hPa: H, U, V, T 300 hPa: H, U, V, T, R, O 400 hPa: H, U, V, T, R, O 500 hPa: H, U, V, T, R, O, Z 600 hPa: H, U, V, T, R, O 700 hPa: H, U, V, T, R, O 850 hPa: H, U, V, T, R, O, X, Y 925 hPa: H, U, V, T, R, O 1,000 hPa: H, U, V, T, R, O Surface: P, U, V, T, R, E†	10 hPa: H, U, V, T 20 hPa: H, U, V, T 30 hPa: H, U, V, T 50 hPa: H, U, V, T 70 hPa: H, U, V, T 100 hPa: H, U, V, T 150 hPa: H, U, V, T 200 hPa: H§, U§, V§, T§, X, Y 250 hPa: H, U, V, T 300 hPa: H, U, V, T, D 400 hPa: H, U, V, T, D 500 hPa: H§, U§, V§, T§, D§, Z 700 hPa: H§, U§, V§, T§, D§, O 850 hPa: H§, U§, V§, T§, D§, O, X, Y 925 hPa: H, U, V, T, D, O 1,000 hPa: H, U, V, T, D Surface: P¶, U¶, V¶, T¶, D¶, E¶	10 hPa: H*, U*, V*, T* 20 hPa: H*, U*, V*, T* 30 hPa: H°, U°, V°, T° 50 hPa: H°, U°, V°, T° 70 hPa: H°, U°, V°, T° 100 hPa: H°, U°, V°, T° 150 hPa: H*, U*, V*, T* 200 hPa: H, U, V, T 250 hPa: H°, U°, V°, T° 300 hPa: H, U, V, T, D*‡ 400 hPa: H*, U*, V*, T*, D*‡ 500 hPa: H, U, V, T, D*‡ 700 hPa: H, U, V, T, D 850 hPa: H, U, V, T, D 1,000 hPa: H, U*, V*, T*, D*‡ Surface: P, U, V, T, D*‡, E†
Forecast hours	0 – 84 every 6 hours and 96 – 192 every 12 hours for 12 UTC † Except analysis	0 – 84 every 6 hours § Additional 96 – 192 every 24 hours for 12 UTC ¶ 0 – 192 every 6 hours for 12 UTC	0 – 72 every 24 hours and 96 – 192 every 24 hours for 12 UTC ° 0 – 120 for 12 UTC † Except analysis * Analysis only
Initial times	00, 06, 12, 18 UTC	00, 06, 12, 18 UTC	00 UTC, 12 UTC ‡ 00 UTC only

Model	Global Ensemble Forecast (One-week)	Ocean Wave Model
Destination	GISC	GTS, GISC
Area and resolution	Whole globe, 2.5° × 2.5°	75°S – 75°N, 0°E – 359.5°E 0.5° × 0.5°
Levels and elements	250 hPa: μU, μV, σU, σV 500 hPa: μH, σH 850 hPa: μU, μV, μT, σU, σV, σT 1,000 hPa: μH, σH Surface: μP, σP	Surface: J, M, G
Forecast hours	0 – 192 every 12 hours	0 – 84 every 6 hours, 96 – 192 every 12 hours for 12 UTC
Initial times	00 UTC and 12 UTC	00 UTC, 06 UTC, 12 UTC, 18 UTC

4.2.4 Operational techniques for application of NWP products

4.2.4.1 In operation

(1) Forecast guidance

The application techniques for both the medium- and short-range forecasting systems are described in 4.3.4.1 (1).

4.2.4.2 Research performed in this field

4.2.5 Ensemble Prediction System (EPS)

4.2.5.1 In operation

The Global EPS (GEPS) has been in operation for medium- to extended-range forecasting since the first quarter of 2017, supporting seamlessly the issuance of five-day tropical cyclone (TC) forecasts, one-week forecasts, early warning information on extreme weather and one-month forecasts. The specifications of GEPS for the first 11 days of forecasts are shown in Table 4.2.5.1-1. The system involves the application of 1 control forecast and 26 perturbed forecasts. Initial perturbations are generated using a combination of the Local Ensemble Transform Kalman Filter approach (LETKF; Hunt et al., 2007) and the singular vector (SV) method (Buizza and Palmer, 1995). LETKF-based initial perturbations representing flow-dependent uncertainty in the initial conditions are produced from LETKF used in an early analysis for global analysis. The tangent-linear and adjoint models used for SV computation are lower-resolution versions of those used in the 4D-Var data assimilation system for the GSM until May 2017. The moist total energy norm (Ehrendorfer et al., 1999) is employed for the metrics of perturbation growth. The forecast model used in the EPS is a low-resolution version of the GSM2003 (see Table 4.2.5.1-1). Accordingly, the dynamical framework and physical processes involved are identical to those in the high-resolution GSM. A stochastic physics scheme (Palmer et al., 2009) is used in GEPS in consideration of model uncertainties associated with physical parameterizations.

Unperturbed initial condition is performed by interpolating the analyzed field in global analysis (see 4.2.1.1). Sea surface temperature (SST) for lower-boundary conditions is spatially interpolated from the SST analysis value at the initial time, and is later prescribed using a two-tiered SST approach (Takakura and Komori, 2020). SST is prescribed using the persisting anomaly from the climatological value for the first 11 days and relaxed from anomaly-fixed SST to the ensemble mean SST of the seasonal EPS (see 4.7.1) linearly from day 12 to day 18 exclusively to the tropics and subtropics. Sea ice concentration for lower-boundary conditions is also based on the analysis value at the initial time, and is prescribed using the persisting anomaly during the forecast range. A perturbation technique for SST that is designed to represent uncertainty in the prescribed SST is applied to GEPS as a surface boundary perturbation.

Table 4.2.5.1-1 Global EPS specifications for the first 11 days of forecasts

1. Ensemble system	
Ensemble (version)	Global EPS (GEPS)
Date of implementation	19 January 2017
2. EPS configuration	
Model (version)	Global Spectral Model (GSM2003)
Horizontal resolution/grid spacing	Spectral triangular 479 (TL479), reduced Gaussian grid system, roughly equivalent to 0.375 × 0.375° (40 km) in latitude and longitude
Vertical resolution (model top)	100 stretched sigma pressure hybrid levels (0.01 hPa)
Forecast length (initial time)	11 days (00, 12 UTC) 132 hours (06, 18 UTC)
Members	1 unperturbed control forecast and 26 perturbed ensemble members
Coupling to ocean/wave/sea ice models	None
Integration time step	720 seconds
Additional comments	None
3. Initial conditions and perturbations	
Initial perturbation strategy	Singular vectors (SVs) and LETKF
Optimization time in forecast for SV	Among three targeted SV areas: 48 hours for Northern Hemisphere (30° – 90°N) 24 hours for Tropics (30°S – 30°N) 48 hours for Southern Hemisphere (90° – 30°S)
Horizontal resolution of perturbations	SVs: Spectral triangular 63 (TL63), reduced Gaussian grid system, roughly equivalent to 2.8125 × 2.8125° (270 km) in latitude and longitude Perturbations from LETKF: See the specifications of LETKF in GA (Table 4.2.1.1 (1)-2).
Initial perturbation area	Global
Data assimilation method for control analysis	Four-dimensional variational (4D-Var) for Global Analysis (GA) Control analysis based on interpolation of high-resolution GA (TL959)
Initial conditions for perturbed members	Addition of perturbations to control analysis (SV-based components in +/- pairs)
Additional comments	LETKF-based perturbations are produced using a total of 26 six-hour forecasts starting from the previous LETKF cycle.
4. Model uncertainty perturbations	
Model physics perturbations	Stochastic perturbation of physics tendency
Model dynamics perturbations	None
Additional comments	· Identical model versions for all ensemble members · Above model uncertainty perturbations not applied to control forecasting
5. Surface boundary perturbations	
Sea surface temperature perturbations	Perturbations representing climatological distribution of analysis and forecast error of prescribed SST sampled from past realizations of

	analysis increment and forecast error of SST in the same season
Soil moisture perturbations	None
Surface wind stress/roughness perturbations	None
Other surface perturbations	None
Additional comments	The above surface perturbations are not applied to the control forecast.
6. Other model details	
Surface boundary conditions	
Treatment of sea surface	Climatological sea surface temperature with daily analysis anomaly Climatological sea ice concentration with daily analysis anomaly
Land surface analysis	Snow depth: two-dimensional optimal interpolation scheme Temperature: first guess Soil moisture: climatology
Model dynamics and physics	
Land surface and soil	Simple Biosphere (SiB) model
Radiation	Two-stream with delta-Eddington approximation for shortwave (hourly) Two-stream absorption approximation method for longwave (hourly)
Numerical techniques	Spectral (spherical harmonic basis functions) in horizontal, finite differences in vertical Two-time-level, semi-Lagrangian, semi-implicit time integration scheme Hydrostatic approximation
Planetary boundary layer	Mellor and Yamada level-2 turbulence closure scheme Similarity theory in bulk formulae for surface layer
Convection	Prognostic Arakawa-Schubert cumulus parameterization
Cloud	PDF-based cloud parameterization
Subgrid orography	Low-level blocked-flow drag, gravity wave drag and turbulent orographic form drag schemes
Non-orographic gravity wave drag	Spectral gravity wave-forcing scheme
7. Products	
Method of calculation (if not unique)	None
Other specifications as necessary	None
8. Further information	
Operational contact	globalnwp@met.kishou.go.jp
System documentation URL	https://www.jma.go.jp/jma/jma-eng/jma-center/nwp/nwp-top.htm

4.2.5.2 Research performed in this field

(1) 2021 GEPS upgrade research

JMA plans to upgrade GEPS in 2021 to incorporate recent GSM developments, an increased ensemble size and improved initial perturbations. The forecast model will be upgraded to a low-resolution version of the newly revised Global Spectral Model (GSM; Ujiie et al., 2021). The ensemble size will be increased from 27 to 51. Singular vector (SV)-based initial perturbations will be improved by (1) implementing up to 50 modes as opposed to the 25 modes of the operational system for each target area of the Northern Hemisphere (30 – 90°N) and the Southern Hemisphere (90 – 30°S), (2) adjustment of amplitude for initial perturbation, and (3) modification of the total SV energy norm

with contributions from above 50 hPa discarded to avoid SV computation with a large peak of energy in the upper stratosphere. To verify system performance for medium-range forecasts with lead times of up to 11 days, retrospective forecast experiments covering periods of three months or more in summer 2019 and winter 2019/20 were conducted. The results showed improved CRPS performance for several elements, including 850 hPa temperature, 500 hPa geopotential height and 250 hPa winds, in the mid-latitudes for both seasons. Brier skill scores for precipitation forecasts in Japan were also improved. Overestimation of ensemble spread for 500-hPa geopotential height forecasts in the mid-latitudes at lead times of around 24 to 72 hours and ensemble mean forecast errors were reduced. See Yamaguchi et al. (2021) for more details.

4.2.5.3 Operationally available EPS products

See 4.2.3.

4.3 Short-range forecasting system (0 – 72 hrs)

4.3.1 Data assimilation, objective analysis and initialization

4.3.1.1 In operation

(1) Meso-scale Analysis (MA)

Meso-scale Analysis (MA) produces initial conditions for the Meso-Scale Model (MSM, 4.3.2.1 (1)). In March 2002, a four-dimensional variational (4D-Var) scheme was introduced as the data assimilation approach for MA (Ishikawa and Koizumi 2002). Following the upgrade of the MSM forecast model to a non-hydrostatic type, MA was replaced by a non-hydrostatic model-based 4D-Var system known as the JMA non-hydrostatic model (JMA-NHM; Saito et al., 2006, 2007) variational data assimilation (JNoVA; Honda et al., 2005) system in April 2009. The further-upgraded ASUCA forecast model (Aranami et al., 2015) has been employed since February 2017, and a 4D-Var system based on ASUCA has been employed since March 2020 (Ikuta et al., 2020). The specifications of MA are described in Table 4.3.1.1 (1)-1.

Table 4.3.1.1 (1)-1 Specifications of the Meso-scale Analysis (MA)

Analysis time	00, 03, 06, 09, 12, 15, 18 and 21 UTC
Analysis scheme	Incremental 4D-Var using a tangent linear forward model in the inner step with low resolution
Data cut-off time	50 minutes for analysis at 00, 03, 06, 09, 12, 15, 18 and 21 UTC
First guess	3-hour forecast produced by ASUCA
Domain configuration (Outer step) (Inner step)	Japan and its surrounding area Lambert projection; 5 km at 60°N and 30°N, 817 × 661 Grid point (1, 1) is at the northwest corner of the domain. Grid point (565, 445) is at 140°E, 30°N. Lambert projection; 15 km at 60°N and 30°N, 273 × 221 Grid point (1, 1) is at the northwest corner of the domain.

	Grid point (189, 149) is at 140°E, 30°N.
Vertical coordinate	z-z* hybrid
Vertical levels	(Outer step) 76 levels up to 22 km (Inner step) 38 levels up to 22 km
Analysis variables	Wind, potential temperature, surface pressure and pseudo-relative humidity, skin temperature, ground temperature and soil moisture
Observations (as of 31 December 2018)	SYNOP, SHIP, BUOY, TEMP, PILOT, Wind Profiler, Weather Doppler radar (radial velocity, reflectivity), AIREP, AMDAR, Typhoon Bogus; AMVs from Himawari-8; ocean surface wind from Metop-A, B/ASCAT; radiances from NOAA-15, 18, 19/ATOVS, Metop-A, B/ATOVS, Aqua/AMSU-A, DMSP-F17, 18/SSMIS, GCOM-W/AMSR2, GPM-core/GMI, WV-CSR of Himawari-8; radar-raingauge analyzed precipitation; precipitation retrievals from DMSP-F17, 18/SSMIS, GCOM-W/AMSR2, GPM-core/GMI, GPM-core/DPR; GNSS RO refractivity data from Metop-A, B/GRAS, COSMIC/IGOR, TerraSAR-X/IGOR, TanDEM-X/IGOR; total precipitable water vapor from ground-based GNSS
Assimilation window	3 hours
System documentation URL	https://www.jma.go.jp/jma/jma-eng/jma-center/nwp/nwp-top.htm

(2) Typhoon bogussing of the MA

The method employed is essentially as per that used for GA (see 4.2.1.1 (2)).

(3) Local Analysis (LA)

Local Analysis (LA) produces initial conditions for the Local Forecast Model (LFM, 4.3.2.1 (2)). Its operation started in August 2012. To provide high-resolution initial conditions that are suitable for LFM, LA is designed to allow rapid production and frequent updating of analysis with a grid spacing of 5 km. In each LA run, an analysis cycle with hourly three-dimensional variational (3D-Var) data assimilation is executed for the previous three hours to incorporate information from newly received observational data in each case. The analysis cycle was originally based on JMA-NHM (Saito et al., 2006, 2007) and the 3D-Var version of JNoVA (Honda et al., 2005), which was replaced by the new-generation 3D-Var version based on ASUCA in January 2015 (Aranami et al., 2015). The capacity of high-resolution NWP to capture small-scale variations in topography is expected to help reduce representativeness errors in the assimilation of surface observations. In association, LA also assimilates Automated Meteorological Data Acquisition System (AMeDAS) data in order to appropriately reflect the effects of local-scale environments near the surface. The specifications of LA are described in Table 4.3.1.1 (3)-1.

Table 4.3.1.1 (3)-1 LA specifications

Analysis time	00, 01, 02, 03, 04, 05, 06, 07, 08, 09, 10, 11, 12, 13, 14, 15, 16, 17, 18, 19, 20,21, 22 and 23 UTC
Analysis cycle	The three-hour analysis cycle repeats hourly assimilation with 3D-Var and one-hour forecasts.
Data cut-off time	30 minutes for analysis at 00, 01, 02, 03, 04, 05, 06, 07, 08, 09, 10, 11, 12, 13, 14, 15, 16, 17, 18, 19, 20, 21, 22 and 23 UTC
First guess	Initial fields produced by the latest MSM

Domain configuration	Japan and its surrounding area Lambert projection; 5 km at 60°N and 30°N, 633 × 521 Grid point (1, 1) is at the northwest corner of the domain. Grid point (449, 361) is at 140°E, 30°N
Vertical coordinate	z-z* hybrid
Vertical levels	48 levels up to 22 km
Analysis variables	Wind, potential temperature, surface pressure, pseudo-relative humidity, skin temperature, ground temperature and soil moisture
Observations (as of 31 December 2018)	SYNOP, SHIP, BUOY, AMeDAS, TEMP, PILOT, Wind Profiler, Weather Doppler radar (radial velocity, reflectivity), AIREP, AMDAR; AMVs from Himawari-8; radiances from NOAA-15, 18, 19/ATOVS, Metop-A, B/ATOVS, Aqua/AMSU-A, DMSP-F17, 18/SSMIS, GCOM-W/AMSR2, GPM-core/GMI, WV-CSRs of Himawari-8; soil moisture from GCOM-W/AMSR2, Metop-A B/ASCAT; total precipitable water vapor from ground-based GNSS
System documentation URL	https://www.jma.go.jp/jma/jma-eng/jma-center/nwp/nwp-top.htm

4.3.1.2 Research performed in this field

(1) Operational use of surface-sensitive clear-sky radiance data in JMA's local NWP system

JMA began to assimilate Himawari-8 surface-sensitive band 9 and 10 (6.9 and 7.3 μm) clear-sky radiance (CSR) data in its local NWP system on July 29 2020 in addition to band 8 (6.2 μm) CSR data (Okabe, 2021). In the quality control process, radiative transfer calculation as implemented in JMA's global NWP system (Okabe, 2019b) and mesoscale NWP system (Okabe, 2019a) was applied. Radiative transfer calculation involves utilization of the land surface emissivity atlas and retrieved land surface temperatures from the window band (10.8 μm; band 13) CSR for better simulated brightness temperature accuracy, especially for surface-sensitive bands. Positive impacts on water vapor and temperature field accuracies for the first guess were shown in the assimilation experiment, which also revealed slightly improved precipitation forecasting scores for heavy rain.

4.3.2 Model

4.3.2.1 In operation

(1) Meso-Scale Model (MSM)

The MSM operated by JMA since March 2001 plays major roles in disaster prevention and aviation forecasting. JMA-NHM (Saito et al., 2006, 2007) was adopted for the MSM in September 2004, and 15- or 33-hour forecasts have been provided every three hours (i.e., eight times a day) since May 2007. The forecast domain was expanded in March 2013. The forecast range at all the initial times was extended to 39 hours in May 2013. The ASUCA forecast model (Ishida et al., 2009, 2010) was introduced in February 2017, and the number of vertical layers was increased from 48 to 76 for enhanced resolution. The forecast range at the initial times of 00 and 12 UTC was extended to 51 hours in March 2019. MSM specifications are listed in Table 4.3.2.1 (1)-1.

Table 4.3.2.1 (1)-1 MSM specifications

1. System	
System	Meso-scale model
Date of implementation	1 March 2001
2. Configuration	
Domain	Japan and its surrounding area Lambert projection, 817 × 661 grid points
Horizontal resolution	5 km at 60°N and 30°N (standard parallels)
Vertical levels	76
Model top	22 km
Forecast length	51 hours (00, 12 UTC), 39 hours (03, 06, 09, 15, 18, 21 UTC)
Runs per day (times in UTC)	8 (00, 03, 06, 09, 12, 15, 18 and 21 UTC)
Coupling to ocean/wave/sea ice models	None
Integration time step	100/3 seconds (3-stage Runge-Kutta method)
3. Surface boundary conditions	
Sea-surface temperature	Analyzed SST and sea-ice distribution
Land surface analysis	Climatological values of evaporability, roughness length and albedo Snow cover analysis over Japan using a land surface model
4. Lateral boundary conditions	
Model providing lateral boundary conditions	GSM
Lateral boundary condition update frequency	4 times/day 00 – 57-hour GSM forecasts initialized at 00/06/12/18 UTC for (03, 06)/(09, 12)/(15, 18)/(21, 00) UTC forecasts
5. Other details	
Soil scheme	Ground temperature prediction using an eight-layer ground model Evaporability prediction initialized using climatological values depending on location and season
Radiation	Short wave: two-stream with delta-Eddington approximation (every 15 minutes) Long wave: two-stream absorption approximation method (every 15 minutes)
Large-scale dynamics	Finite volume method with Arakawa-C-type staggered coordinates, horizontally explicit and vertically implicit time integration scheme, and combined third- and first-order upwind horizontal finite difference schemes in flux form with a limiter as proposed by Koren (1993) in advection treatment for monotonicity, time-splitting of vertical advection Fully compressible non-hydrostatic equations
Boundary layer	Mellor-Yamada-Nakanishi-Niino Level-3 scheme Similarity theory adopted for surface boundary layer
Convection	Kain-Fritsch convection scheme
Cloud/microphysics	Three-ice bulk cloud microphysics Consideration of PDF-based cloud distribution in microphysics Time splitting of vertical advection for water substances, cloud water and cloud cover diagnosed using a partial condensation scheme
Orography	Mean orography smoothed to eliminate shortest-wave components
Horizontal diffusion	None
Gravity wave drag	None
6. Further information	
System documentation URL	https://www.jma.go.jp/jma/jma-eng/jma-center/nwp/nwp-top.htm

(2) Local Forecast Model (LFM)

JMA has operated LFM since August 2012. The model has a 2-km horizontal grid spacing and 58 vertical layers up to a height of approximately 20 km above the surface with a nine-hour forecast range, and is designed to produce detailed forecasts with emphasis on predicting localized and short-lived severe events. The main purposes of the LFM are to provide very short-range forecasts and to allow rapid and frequent forecast updates based on initial conditions with the latest observations assimilated via LA (4.3.1.1 (3)). The forecast domain was expanded to cover Japan and its surrounding areas, and the update frequency was enhanced to every hour in May 2013. The ASUCA forecast model was introduced in January 2015 (Aranami et al., 2015), replacing the previous JMA-NHM (Saito et al., 2006, 2007). The forecast range for all the initial times was extended to 10 hours in March 2019. The specifications of the LFM are listed in Table 4.3.2.1 (2)-1.

Table 4.3.2.1 (2)-1 LFM specifications

1. System	
System	Local Forecast Model
Date of implementation	30 August 2012
2. Configuration	
Domain	Japan and its surrounding area Lambert projection, 1,581 × 1,301 grid points
Horizontal resolution	2 km at 60°N and 30°N (standard parallels)
Vertical levels	58
Model top	20 km
Forecast length	10 hours
Runs per day (times in UTC)	24 (00, 01, 02, 03, 04, 05, 06, 07, 08, 09, 10, 11, 12, 13, 14, 15, 16, 17, 18, 19, 20, 21, 22 and 23 UTC)
Coupling to ocean/wave/sea ice models	None
Integration time step	50/3 seconds (3-stage Runge-Kutta method)
3. Surface boundary conditions	
Sea-surface temperature	Analyzed SST and sea-ice distribution
Land surface analysis	Climatological values of evaporability, roughness length and albedo Snow cover analysis from MSM
4. Lateral boundary conditions	
Model providing lateral boundary conditions	MSM
Lateral boundary condition update frequency	8 times/day 00 – 13-hour forecasts using the latest MSM information
5. Other details	
Soil scheme	Ground temperature prediction using an eight-layer ground model Evaporability prediction initialized using climatological values depending on location and season
Radiation	Short wave: two-stream with delta-Eddington approximation (every 15 minutes) Long wave: two-stream absorption approximation method (every 15 minutes)
Large-scale dynamics	Finite volume method with Arakawa-C-type staggered coordinates, horizontally explicit and vertically implicit time integration scheme, and combined third- and first-order upwind horizontal finite difference schemes in flux form with a limiter as proposed by Koren (1993) in advection treatment for monotonicity, time-splitting of vertical advection

	Fully compressible non-hydrostatic equations
Boundary layer	Mellor-Yamada-Nakanishi-Niino Level 3 scheme Similarity theory adopted for surface boundary layer
Convection	Convective initiation
Cloud/microphysics	Three-ice bulk cloud microphysics Time splitting of vertical advection for water substances Cloud water and cloud cover diagnosis using a partial condensation scheme
Orography	Mean orography smoothed to eliminate shortest-wave components
Horizontal diffusion	None
Gravity wave drag	None
6. Further information	
System documentation URL	https://www.jma.go.jp/jma/jma-eng/jma-center/nwp/nwp-top.htm

4.3.2.2 Research performed in this field

4.3.3 Operationally available NWP products

4.3.4 Operational techniques for application of NWP products

4.3.4.1 In operation

(1) Forecast guidance

Forecast guidance is utilized for the issuance of warnings, advisories, information and weather forecasts. The operational techniques routinely used to determine guidance from NWP model output are Kalman Filter (KF), Neural Network (NN), Multiple Linear Regression (MLR), Logistic Regression (LR), Diagnostic Methods (DM), and Lagged Average Forecast (LAF). These approaches are applied to grid-point values from GSM, MSM, LFM, and MEPS in order to reduce systematic errors in NWP models and to extract useful information such as probabilities and categorical/diagnostic values. The specifications of weather forecast guidance and aviation forecast guidance are listed in Tables 4.3.4.1 (1)-1 and 4.3.4.1 (1)-2, respectively.

Table 4.3.4.1 (1)-1 Weather forecast guidance specifications

Guidance based on GSM data is provided every 6 hours with forecast lead times between 3 and 84 hours every 3 hours. Guidance based on MSM data is provided every 3 hours with forecast times between 3 and 39 hours (51 hours for 00, 12 UTC initial) every 3 hours. Guidance based on LFM data is provided every hour with forecast lead times between 1 and 10 hours every hour.

Element	Details	Type	NWP	Statistical tool
Average precipitation	Mean precipitation amount over 3 hours (grid average)	Grid (20 * 20 km for GSM, 5 * 5 km for MSM and MEPS)	GSM, MSM, MEPS	KF
Maximum precipitation	Maximum precipitation (within each grid square) over 1, 3, 12, 24, 48 and 72 hours (48 and 72 hours for GSM only)			NN (1, 3 hours), MLR (24 hours)

Probability of precipitation	Probability of precipitation totaling 1 mm or more over 6 hours			KF
Weather	Categorization (including sunshine duration and precipitation type)			NN (sunshine duration), DM (precipitation type)
Visibility	Minimum visibility			DM
Average precipitation	Mean precipitation amount over 1 hour (grid average)	Grid (5 * 5 km for LFM)	LFM	LAF
Maximum precipitation	Maximum precipitation over 1 hour (maximum value within each grid square)			
Maximum snowfall	Snowfall amount over 3, 6, 12 and 24 hours (maximum value within each grid square)	Grid (5 * 5 km)	GSM, MSM, MEPS	DM + LR
Snowfall	Snowfall amount over 6, 12 and 24 hours	Point (323)		NN
Temperature	Maximum, minimum, time-series temperature	Point (928)		KF
Wind	Maximum, time-series wind speed/direction	Point (928)		KF
Humidity	Minimum humidity, time-series humidity	Point (154)		NN (minimum), KF (time series)
Probability of TS	Probability of thunderstorms	Grid (20 * 20 km)		LR

Table 4.3.4.1 (1)-2 Aviation forecast guidance specifications

Guidance based on the MSM is provided every 3 hours with forecast times between 1 and 39 hours (51 hours for 00 and 12 UTC initials) every hour. Guidance based on the LFM is provided every hour with forecast times between 1 and 10 hours every hour.

Element	Details	Type	NWP	Statistical tool
Visibility	Minimum and mean visibility	Point (90 airports)	MSM, MEPS	KF
Probability of visibility	Probability of visibility less than 5,000 and 1,600 m			KF
Cloud	Cloud amount and height of lower 3 layers			NN
Probability of ceiling	Probability of ceiling below 600 and 1,000 ft			LR
Wind	Time-series, maximum wind speed/direction			KF
Gust	Gust speed/direction			KF
Probability of gusts	Probability of gusting			LR
Weather	Categorized weather			DM
Temperature	Maximum, minimum and time-series temperature			KF
Turbulence	Turbulence index	Grid (40 * 40 km and 28 layers for MSM and MEPS, 10 * 10 km and 45	GSM, MSM, LFM, MEPS	LR

Icing	Icing index	layers for LFM)	GSM, MSM, LFM, MEPS	DM
CB	CB cloud amount and CB top height		GSM, MSM, LFM, MEPS	DM
Visibility	Minimum visibility		LFM, MEPS	DM

(2) Hourly Analysis

Hourly Analysis involves three-dimensional evaluation of temperature and wind fields with a grid spacing of 5 km to provide real-time monitoring of weather conditions. The latest MSM forecast is used as the first guess, and observational information is added through data assimilation. The 3D-Var data assimilation method is adopted as the analysis technique, and the hourly product is made and distributed by 30 minutes past the hour. In July 2017, ASUCA data were adopted in a new system and a 3D-Var data assimilation system based on ASUCA (Aranami et al., 2015) was implemented, replacing the original one based on JMA-NHM (Saito et al., 2006, 2007) and JNoVA (Honda et al., 2005). The specifications of Hourly Analysis are listed in Table 4.3.4.1 (2)-1.

Table 4.3.4.1 (2)-1 Hourly Analysis specifications

Analysis time	Every hour on the hour
Analysis scheme	3D-Var
Data cut-off time	18 minutes past the hour
First guess	2, 3 or 4-hour forecast by MSM
Domain configuration	Japan and its surrounding area Lambert projection, 5 km at 60°N and 30°N, 721 × 577 Grid point (1, 1) is at the northwest corner of the domain. Grid point (489, 409) is at 140°E, 30°N.
Vertical coordinates	z-z^* hybrid
Vertical levels	48 levels up to 22 km
Analysis variables	Wind, temperature, surface wind and surface temperature
Observations (as of 31 December 2018)	AMeDAS, Wind Profiler, Weather Doppler radar (radial velocity), AIREP, AMDAR, and AMVs from Himawari-8
Post-processing	Surface filtering (followed by adjustment of the increment within the boundary layer)
Product distribution	By 30 minutes past the hour

4.3.4.2 Research performed in this field

(1) Forecast guidance

JMA's development of guidance for the Tokyo 2020 Olympic and Paralympic Games is based on MSM data, with prediction of temperature and wind at individual competition venues. The Agency also develops heavy-rain probability guidance targeting emergency warning-grade heavy rain (totaling 100 or 150 mm or more over 3 hours) with 5-km grid intervals and seamless multi-model integrated

(MMI) guidance providing accurate, high-resolution prediction up to 5 days ahead for precipitation, wind, temperature and snowfall via integration of multiple NWP outputs and guidance with cutting-edge AI technology.

4.3.5 Ensemble Prediction System (EPS)

4.3.5.1 In operation

The Meso-scale Ensemble Prediction System (MEPS; specifications: Table 4.3.5.1-1) was introduced in June 2019 to provide uncertainty information for the MSM (Ono et al., 2021). It consists of 21 members, including one non-perturbed run, and is used to evaluate forecast uncertainty in consideration of initial and lateral boundary perturbations. Initial perturbations comprise a linear combination of global SVs (GSVs) based on the GSM and mesoscale SVs (MSVs) from JMA-NHM (Ono et al., 2011), which have different spatial and temporal resolutions. Lateral boundary perturbations are supplied from linearly evolved GSVs (Ono, 2017), ensuring consistency between initial and boundary conditions. The total energy norm (Ehrendorfer et al., 1999) is employed for perturbation growth metrics in SV definition. As the forecast model used in each ensemble member is exactly the same as the MSM, non-perturbed control forecast in MEPS is identical to MSM forecast. In September 2020, optimization of initial and lateral boundary perturbations (including adaptive targeting in which a target MSV area is adaptively limited depending on weather conditions) was introduced (Kakehata et al., 2021).

Table 4.3.5.1-1 MEPS specifications

1. System	
System	Meso-scale Ensemble Prediction System
Date of implementation	27 June 2019
2. Configuration	
Domain	Japan and its surrounding area Lambert projection, 817 × 661 grid points
Horizontal resolution	5 km at 60 and 30°N (standard parallels)
Vertical levels	76
Model top	22 km
Forecast length	39 hours
Runs per day (times in UTC)	4 (00, 06, 12 and 18 UTC)
Members	One unperturbed control forecast and 20 perturbed ensemble members
Coupling with ocean/wave/sea ice models	None
Integration time step	100/3 seconds (3-stage Runge-Kutta method)
3. Initial conditions and perturbations	
Initial perturbation strategy	Singular vectors (SVs); linear combination of MSV40s, MSV80s and global SVs (GSVs)
Horizontal resolution of perturbations	MSV40: 40 km MSV80: 80 km GSV: Spectral triangular 63 (TL63), reduced Gaussian grid system, roughly equivalent to 2.8125 × 2.8125° (270 km) in latitude and longitude
Optimization time in forecast	MSV40: 6 hours MSV80: 15 hours GSV: 45 hours

Target area	MSV40: 125 – 145°E, 25 – 45°N MSV80: 125 – 145°E, 25 – 45°N GSV: 120 – 170°E, 25 – 45°N For MSV, grid points with 925 hPa vorticity lower than a certain threshold were removed from the rectangular target area
Data assimilation for control analysis	4D-Var analysis with mixing ratios of cloud water, cloud ice, rain, snow and graupel derived from preceding forecasts in consideration of consistency with analysis field for relative humidity
Initial conditions for perturbed members	Perturbations added to control analysis in +/−pairs
4. Lateral boundary perturbations	
Lateral perturbation strategy	Based on integration of GSV (a large-scale component of initial perturbation) using the tangent linear model
5. Other model details	
	All ensemble members use exactly the same model as the MSM.

4.4 Nowcasting and Very-short-range Forecasting systems (0 – 15 hrs)

Since 1988, JMA has routinely operated a fully automated system of precipitation analysis and very short-range forecasting to monitor and forecast local severe weather conditions. In addition to these, JMA has issued Precipitation Nowcasts since June 2004, Thunder Nowcasts since May 2010 and Hazardous Wind Potential Nowcasts since May 2010. High-resolution Precipitation Nowcasts (JMA's latest nowcasting product) were introduced in August 2014. Extended Very-Short-Range Forecasts of precipitation (ExtVSRF) were introduced in June 2018. Snow Depth and Snowfall Amount Analysis were introduced in November 2019.

The products are listed below.

(1) High-resolution Precipitation Nowcasts (incorporating forecasts of 5-minute cumulative precipitation, 5-minute-interval precipitation intensity and error range estimation based on extrapolation and spatially three-dimensional forecasting covering the period up to 60 minutes ahead)
(2) Precipitation Nowcasts (incorporating forecasts of 10-minute cumulative precipitation and 5-minute-interval precipitation intensity based on extrapolation covering the period up to 60 minutes ahead)
(3) Thunder Nowcasts (incorporating forecasts of thunder and lightning activity based on lightning detection network system observation covering the period up to 60 minutes ahead)
(4) Hazardous Wind Potential Nowcasts (incorporating forecasts of the probability of hazardous wind conditions such as tornadoes covering the period up to 60 minutes ahead)
(5) Radar/Raingauge-Analyzed Precipitation (R/A)* (incorporating one-hour cumulative precipitation based on radar observation calibrated using raingauge measurements from JMA's Automated Meteorological Data Acquisition System (AMeDAS) and other available data such

as those from rain gauges operated by local governments)

(6) Very-Short-Range Forecasts of precipitation (VSRFs) (incorporating forecasts of one-hour cumulative precipitation based on extrapolation and prediction by the MSM and LFM (see 4.3.2.1) including both Guidance (see 4.3.4.1) and covering the period from one to six hours ahead)

(7) Extended VSRF (ExtVSRF) (incorporating forecasts of one-hour cumulative precipitation based on prediction and guidance from the MSM and LFM (see 4.3.2.1) and covering the period from 7 to 15 hours ahead)

(8) Snow Depth and Snowfall Amount Analysis (incorporating analysis of snow depth based on estimates from a model simplifying temporal variations in snow properties modified using snow-depth gauge data from AMeDAS and analysis of snowfall amounts based on the increment between current and previous snow depths)

*Referred to before 15 November 2006, as *Radar-AMeDAS precipitation*.

4.4.1 Nowcasting system (0 – 1 hrs)

4.4.1.1 In operation

(1) High-resolution Precipitation Nowcasts

High-resolution precipitation nowcasts (HRPNs) provide five-minute-interval precipitation intensity and cumulative precipitation data up to an hour ahead. Initial precipitation intensity distribution is determined via three-dimensional analysis of storms using radar echo intensity, Doppler velocity, raingauge, surface and upper-air observation data.

Data on vertical atmospheric profiles are part of the input used for prediction generation. The initial values for such data are based on upper-air observation data, and are updated via comparison of cumulonimbus cloud profiles (echo top rising speed, ceiling height, lightning count and rainfall amount) between radar/radio-based observation and calculation using the Vertically One-dimensional Convective Model (VOCM). Thus, HRPNs are multi-observing-system-based nowcasting products beyond the scope of radar-based data with concentration on various observation data application technologies.

Two processes are adopted in HRPNs: (1) high-resolution three-dimensional prediction generated by extrapolating the three-dimensional distribution of water content and using VOCM data relating to notable regions of heavy rain, and (2) low-resolution three-dimensional prediction generated with a longer time step and reduced vertical calculation for areas outside high-resolution prediction regions. Data processing functions are designed for prediction using a dynamical estimation approach suitable for forecasting of rain phenomena that develop widely and rapidly based on a kinetic

approach involving the extrapolation of phenomenon movement trends. Generation of data on convective cloud initiation triggered by three phenomena is also considered.

HRPN distribution data contain information on prediction uncertainty in the form of predictions regarding the magnitude of errors included in forecast rainfall. Knowledge of this uncertainty is considered useful in applications such as river water level prediction. The specifications are summarized in Table 4.4.1.1 (1)-1. HRPN are provided to local weather offices and the public to enable close monitoring of heavy-rain areas and support disaster prevention activities.

Table 4.4.1.1 (1)-1 High-resolution Precipitation Nowcast model specifications

Forecast process	• Kinetic: non-linear motion/intensity extrapolation • Dynamic: vertically one-dimensional convective model enabling calculation relating to raindrop generation, precipitation and evaporation • Convective Initiation: three triggers: (1) downflow caused by heavy rainfall, (2) temporal variation of surface temperature and water vapor, (3) intersection of arch-shaped thin echo
Movement vector	• Precipitation system, cell and rain intensity trend motion vectors estimated using cross-correlation pattern matching and discrete interpolation • Dual-Doppler wind
Time step	5 minutes (low-resolution three-dimensional prediction) 1 minute (high-resolution three-dimensional prediction) 1 second (vertically one-dimensional convective model)
Grid form	Cylindrical equidistant projection
Resolution and forecast time	Approx. 250 m over land and coasts 00 − 30 minutes ahead 1 km over land and coasts 35 − 60 minutes ahead 1 km from the coasts 00 − 60 minutes ahead
Number of grids	16,660,800 for distribution data, with up to 51,840,000 for internal calculation of high-resolution three-dimensional prediction
Initial	• Analyzed precipitation distribution determined from radar, raingauge and upper-air observation • Vertical atmospheric profiles based on radiosonde and cumulonimbus cloud features
Update interval	Every 5 minutes

(2) Precipitation Nowcasts

Precipitation Nowcasts predict 10-minute accumulated precipitation and 5-minute-interval precipitation intensity by extrapolation up to one hour ahead. Initial precipitation intensity distribution is derived from radar data obtained at 5-minute intervals, and is calibrated by raingauge observation. Using estimated movement vectors, these forecasts predict precipitation distribution on the basis of extrapolation. Calculation takes approximately three minutes. These processes are scheduled to be replaced with the smoothing applied for the output of High-resolution Precipitation Nowcasts. The specifications are summarized in Table 4.4.1.1 (2)-1.

Precipitation Nowcasts are provided to local weather offices and the public to help clarify

precipitation transition and support disaster prevention activities.

Table 4.4.1.1 (2)-1 Precipitation Nowcast model specifications

Forecast process	Non-Linear motion/intensity extrapolation including the generation and lifecycle estimation of storm cells as well as orographic rainfall trend prediction
Movement vector	Precipitation system and/or cell motion estimated using the cross-correlation pattern matching and discrete interpolation
Time step	5 minutes
Grid form	Cylindrical equidistant projection
Resolution	Approx. 1 km
Number of grids	2,560 × 3,360
Initial	Calibrated radar echo intensities
Forecast time	60 minutes ahead, updated every 5 minutes

(3) Thunder Nowcasts

Thunder Nowcasts predict thunder and lightning activity up to an hour ahead. Initial activity distribution is derived from the lightning detection network system, radar data and Himawari-8/9 multiband observation conducted at 10-minute intervals. In consideration of estimated movement vectors, these forecasts predict activity distribution on the basis of extrapolation. Calculation takes approximately three minutes. The specifications are summarized in Table 4.4.1.1 (3)-1.

Thunder Nowcasts are provided to local weather offices and to the public. They are utilized to understand thundercloud transfer and to advise people to stay in or go to safe places in order to avoid lightning strikes.

Table 4.4.1.1 (3)-1 Thunder Nowcast model specifications

Forecast process	Extrapolation
Movement vector	As per the Precipitation Nowcast system
Grid form	Cylindrical equidistant projection
Resolution	Approx. 1 km
Number of grids	2,560 × 3,360
Initial	4-level activity of thunder and lightning based on the lightning detection network system, radar data and Himawari-8/9 high-frequency multiband observation
Forecast time	60 minutes ahead, updated every 10 minutes

(4) Hazardous Wind Potential Nowcasts

Hazardous Wind Potential Nowcasts predict the probability of hazardous wind conditions such as tornadoes up to one hour ahead. Initial probability distribution is established using radar measurements including Doppler radar data obtained at 10-minute intervals and severe weather parameters calculated from Numerical Weather Prediction. Using estimated movement vectors, these forecasts predict probability distribution on the basis of extrapolation. Calculation takes

approximately three minutes. The specifications are summarized in Table 4.4.1.1 (4)-1.
Hazardous Wind Potential Nowcasts are provided to local weather offices and the public to clarify the transition of areas with high potential for hazardous winds and call attention to related hazardous conditions.

Table 4.4.1.1 (4)-1 Hazardous Wind Potential Nowcast model specifications

Forecast process	Extrapolation
Movement vector	As per the Precipitation Nowcast system
Grid form	Cylindrical equidistant projection
Resolution	Approx. 10 km
Number of grids	256 × 336
Initial	2-level presumed hazardous wind probabilities
Forecast time	60 minutes ahead, updated every 10 minutes

4.4.1.2 Research performed in this field

4.4.2 Models for Very-short-range Forecasting Systems (1 – 15 hrs)

4.4.2.1 In operation

(1) Radar/Raingauge-Analyzed Precipitation (R/A)

Radar data and raingauge precipitation data are analyzed every 30 minutes to create Radar/Raingauge Analyzed Precipitation (R/A) information with a resolution of 1 km. This involves the collection of radar echo intensity information from 46 weather radars operated by JMA and the Ministry of Land, Infrastructure, Transport and Tourism (MLIT) and precipitation data from more than 10,000 raingauges operated by JMA, MLIT and local governments.

Radar intensity readings are collected to create one-hour cumulative radar precipitation data, and are calibrated with one-hour cumulative raingauge precipitation data. R/A is a composite of all calibrated and cumulative radar precipitation data. The initial field for extrapolation forecasting is a composite of calibrated radar intensity data.

Dissemination of “Immediate R/A” information every 10 minutes was started in July 2017. This involves the collection of information from the same number of the weather radar and the less number of raingauges in contrast to the “Regular R/A”.

(2) Very-Short-Range Forecasts of precipitation (VSRFs) (1 – 6 hrs)

The extrapolation forecast and precipitation forecast from the MSM and the LFM (see 4.3.2.1) including both Guidance (see 4.3.4.1) are merged into the Very-Short-Range Forecast of precipitation (VSRFs). The merging weight of the MSM/LFM forecast is nearly zero for a one-hour forecast, and

is gradually increased with forecast time to a value determined from the relative skill of MSM/LFM forecasts. The specifications of the extrapolation model are detailed in Table 4.4.2.1 (2)-1.

Table 4.4.2.1 (2)-1 Extrapolation model specifications used in VSRFs

Forecast process	Extrapolation
Physical process	Enhancement and dissipation
Movement vector	Precipitation system movement evaluated using the cross-correlation method
Time step	2 – 5 minutes
Grid form	Oblique conformal secant conical projection
Resolution	1 km
Number of grids	1,600 × 3,600
Initial	Calibrated radar echo intensities
Forecast time	Up to six hours from each initial time (every 10 minutes = 144 times/day)

Following on from the introduction of Immediate R/A data in 2017, JMA began providing Immediate VSRF data in March 2018. This information is issued every 10 minutes to support local weather offices that issue warnings for heavy precipitation, and is used for forecast calculation relating to applied products such as the Soil Water Index and the Runoff Index.

(3) Extended Very-Short-Range Forecasts of precipitation (ExtVSRF) (7 – 15 hrs)

In June 2018, JMA launched its extended ExtVSRF forecast to support early judgement regarding the need for evacuation and other measures by clarifying the tendency of rainfall toward dawn when heavy rain falls in the evening. This forecast facilitates understanding of overall precipitation distribution as a trend, and was developed as a separate product from VSRF.

The forecast is derived from a combination of MSM precipitation amount forecasts, MSM Guidance for mean and maximum precipitation amounts and LFM Guidance for maximum precipitation amounts, and is not merged with EX6 data because the latter's precision from 7 to 15 hours ahead is significantly poorer than that produced by the combination of these guidance forecasts.

The latest available guidance forecasts for mean and maximum precipitation are divided into two groups and verified with current analysis R/A using the Fractions Skill Score (FSS). The forecast with the best score from each group is chosen and mixed with the weighted average.

Table 4.4.2.1 (3)-1 Forecast model specifications used in ExtVSRF

Forecast process	Combination of MSM precipitation amount forecasts, MSM Guidance for mean and maximum precipitation amounts and LFM Guidance for maximum precipitation amounts
Combination process	Verified with current analysis R/A using the Fractions Skill Score (FSS)
Grid form	Oblique conformal secant conical projection
Resolution	5 km
Number of grids	320 × 720
Forecast time	From seven to fifteen hours from each initial time (every hour = 24 times/day)

4.4.2.2 Research performed in this field

4.4.3 Snow Analysis System (0 hrs)

4.4.3.1 In operation

(1) Snow Depth and Snowfall Amount Analysis

The Snow Depth and Snowfall Amount Analysis products support mapping of snow depths and snowfall amounts, including for areas where snow depth observation is not conducted, and are issued every hour with a spatial resolution of 5 km.

Snow Depth Analysis is based on a model simplifying temporal variations in snow properties and is modified using AMeDAS snow gauge measurements. The model estimates snow depth based on fresh accumulation, melting and settling over time with R/A precipitation and, precipitation, temperature and solar radiation from the LFM as inputs. Optimum interpolation is used to modify estimated snow depths.

Snowfall Amount Analysis is based on the increment between current and previous snow depths. For values lower than previous data, a zero input is recorded.

Table 4.4.3.1 (1)-1 Snow Depth and Snowfall Amount Analysis specifications

Analysis process	Snow Depth Analysis is estimated using a model simplifying temporal variations in snow properties, modified using snow depth gauge measurements from AMeDAS. Snowfall Amount Analysis is based on the increment between current and previous snow depths.
Grid form	Cylindrical equidistant projection
Resolution	5 km
Number of grids	560 × 512
Analysis time	Every hour

4.4.3.2 Research performed in this field

4.5 Specialized numerical predictions

4.5.1 Assimilation of specific data, analysis and initialization (where applicable)

4.5.1.1 In operation

(1) Global Ocean Data Assimilation System

JMA's global ocean data assimilation system was upgraded in June 2015 to the MOVE/MRI.COM-

G2 version (Toyoda et al., 2013) developed by its Meteorological Research Institute. Its specifications are shown in Table 4.5.1.1 (1)-1.

The outputs of MOVE/MRI.COM-G2 are used to monitor and diagnose tropical ocean status. Some figures based on MOVE/MRI.COM-G2 output are published in JMA's *Monthly Highlights on Climate System* and provided through the Tokyo Climate Center (TCC) website (https://ds.data.jma.go.jp/tcc/tcc/index.html). The data are also used as oceanic initial conditions for the seasonal EPS (JMA/MRI- CPS2).

Table 4.5.1.1 (1)-1 Global ocean data assimilation system specifications

System version	MOVE/MRI.COM-G2	MOVE/MRI.COM-G3	
		G3A (Low-resolution 4DVAR)	G3F (High-resolution Downscaling)
Operation start date	June 2015	January 2022 (TBD)	
Basic equations	Primitive with free surface, solved via finite difference consideration		
Resolution	1 (longitude) × 0.3 – 0.5° (latitude)	1 (longitude) × 0.3 – 0.5° (latitude)	0.25 (longitude) × 0.25° (latitude)
	52 vertical levels with a bottom boundary layer	60 vertical levels with a bottom boundary layer	60 vertical levels
Observational data	Sea-surface and subsurface temperature, salinity and sea surface height	Sea-surface and subsurface temperature, salinity, sea surface height and sea ice concentration	Sea ice concentration
Assimilated gridded SST product	COBE-SST	MGDSST	
Analysis method	3DVAR-FGAT IAU	4DVAR IAU	IAU towards G3A temperature and salinity
Sea ice DA		Sea ice cover 3DVAR	
Atmospheric forcing	JRA-55 Reanalysis	JRA-3Q + Global Analysis	JRA-3Q + Global Analysis
Analysis window	10 days	10 days (5 for IAU plus 5 for data assimilation)	5 days
Update frequency	Every five days (two staggered streams)	Every day (five staggered streams)	
Operational runs	Two (final and early) with cut-off times of 33 and 2 days for ocean observation data	Two (final and early) with cut-off times of 4 days and several hours for ocean observation data	

(2) High-resolution sea surface temperature analysis for global oceans and the western North Pacific

Since 2005, JMA has operated a sea surface temperature (SST) analysis system to generate global daily 1/4° × 1/4° grid SST data (merged satellite and in-situ data Global Daily Sea Surface Temperature, or MGDSST). The system involves the use of an optimal interpolation (OI) approach with consideration of spatial and temporal correlation. SST data obtained from polar-orbiting satellites (AVHRRs on the NOAA series and Metop/AMSR2 on GCOM-W) are used in the OI together with in-situ SST observations. MGDSSTs are used for ocean information services at JMA, for boundary conditions in short-to medium-range NWP models, and for observational data in ocean data assimilation for the North Pacific Ocean.

The HIMSST (High-resolution Merged Satellite and In-situ Data Sea Surface Temperature) analysis product, providing regional daily high-resolution (1/10˚ × 1/10˚) analysis for the western North Pacific, was introduced in November 2016 with an analysis framework based on that of MGDSST along with components of smaller spatial and shorter temporal scales derived from Himawari-8 L3 SST (Kurihara et al., 2016). It has been used to provide boundary conditions for short-range NWP models, such as the Meso-Scale Model (MSM) and the Local Forecast Model (LFM), since March 2019.

The analysis data are available on the NEAR-GOOS Regional Real Time Database (https:// www.data.jma.go.jp/goos/data/database.html).

(3) Ocean wave analysis

A wave data assimilation system for JMA's operational wave model was put into operation in October 2012. The system is described below.
1) Wave data are not assimilated directly; the system refers to analysis wave heights of the JMA Objective Wave Analysis System (OWAS). The specifications are shown in Table 4.5.1.1 (3)-1. The key factor for rectification is the ratio of wave heights between model products and OWAS products.
2) In modification, windsea and swell parts are extracted and modified. Windsea spectra are modified based on the JONSWAP spectrum profile, and the peak frequency is determined in consideration of Toba's power law. For swell spectrum modification, the system rescales swell spectrum by the ratio of wave heights between model products and OWAS products. For details of the wave analysis system, refer to Kohno et al. (2012).

Table 4.5.1.1 (3)-1 JMA Objective Wave Analysis System (OWAS) specifications

Analysis scheme	Optimal interpolation
Data cut-off time	6 hours and 25 minutes for early-run analysis 12 hours for delayed analysis
First guess	6-hour forecast by the GWM
Analysis variables	Significant wave height
Grid size	0.5˚ (longitude) × 0.5˚ (latitude)
Integration domain	Global oceans

Observational data	BUOY, SHIP, Nowphas, GPS wave meter, JASON3, SARAL, Sentinel-3A/B
Assimilation window	6 hours

4.5.1.2 Research performed in this field

(1) Implementation of MOVE/MRI.COM-G3

JMA's new MOVE/MRI.COM-G3 global ocean data assimilation system (Table 4.5.1.1 (1)-1) will be assessed in the coming years along with long-term ocean re-analysis in tandem with ongoing JRA-3Q production. The system incorporates low-resolution 4DVAR analysis (G3A) for tropical-ocean monitoring as before, along with an eddy-permitting resolution downscaling run (G3F) for ocean model initialization in JMA/MRI-CPS3 (see 4.7.1). Data assimilation will be upgraded from 3DVAR to 4DVAR to give a more dynamically consistent initial state with the model. Sea ice concentration will also be assimilated with 3DVAR. This is expected to further improve forecasts for polar regions.

(2) Operational use of Sentinel-3A/B significant wave height data in JMA ocean wave analysis

JMA began to assimilate significant wave height data from the SAR Radar Altimeter (SRAL) equipment on Sentinel-3A and 3B into its ocean wave analysis system in September 2020, in addition to data from Jason-3 and Saral.

4.5.2 Specific models

4.5.2.1 In operation

(1) Environmental emergency response system

JMA acts as a Regional Specialized Meteorological Center (RSMC) for Environmental Emergency Response in WMO Regional Association (RA) II, and is responsible for the preparation and dissemination of transport model products on exposure and surface contamination involving accidentally released radioactive materials. An operational tracer transport model is run at the request of National Meteorological Services in RA II and the International Atomic Energy Agency (IAEA) to offer RSMC support for environmental emergency response.

A Lagrangian method is adopted for the transport model, and large numbers of tracers are released at certain times and locations in line with pollutant emission information provided as part of related requests. Effects on three-dimensional advection and horizontal/vertical diffusion, dry and wet deposition and radioactive decay are computed from three-hourly outputs of the high-resolution global model (TL959L100). The standard products of the RSMC involve maps on trajectories, time-integrated low-level concentrations and total deposition up to 72 hours ahead.

As part of the CTBTO-WMO Backtracking Response System, JMA is responsible for providing

atmospheric backtracking products to the Comprehensive Nuclear-Test-Ban Treaty Organization (CTBTO) in its role as a Regional Specialized Meteorological Center. JMA developed an atmospheric backtracking transport model and built up a response system that receives e-mail notifications from CTBTO, executes backtracking calculations and provides the resulting products in line with the procedure defined in WMO no. 485. JMA began operation of the backtracking system in December 2009. Backtracking over a period up to 50 days can be provided on an operational basis.

(2) Ocean-wave forecasting models

JMA operates four numerical wave models: the Global Wave Model (GWM), the Coastal Wave Model (CWM), the Wave Ensemble System (WENS), and the Shallow-water Wave Model (SWM). The GWM, CWM and WENS are based on MRI-III, which was developed at JMA's Meteorological Research Institute (MRI), and a major update was made to the current version in May 2007. The WENS has been operational since June 2016, and was upgraded in March 2020 with enhancement of horizontal resolution from 1.25° to 0.5° in both longitude and latitude and the implementation of shallow-water effects. The specifications of the models are given in Table 4.5.2.1 (2)-1.

JMA began calculating wave components (windsea and swell) for the GWM and CWM on 20 July 2016. Since the upgrade of JMA's supercomputer system on 5 June 2018, the forecast lengths of the GWM and CWM initialized at 00, 06 and 18 UTC have been extended from 84 to 132 hours, and the model run frequency of the WENS has been increased from once to twice a day.

The SWM is based on the WAM, which was modified at the National Institute for Land and Infrastructure Management of MLIT and put into operation under a cooperative framework with MLIT's Water and Disaster Management Bureau. The model is applied to 22 sea areas along the coast of Japan. The models' specifications are given in Table 4.5.2.1 (2)-2.

Table 4.5.2.1 (2)-1 Ocean-wave prediction model specifications

Model name	Global Wave Model	Coastal Wave Model	Wave Ensemble System
Model type	Spectral model (third-generation wave model)		
Date of implementation	May 2007	May 2007	March 2020
Grid form	Equal latitude-longitude grid on spherical coordinates		
Grid interval	0.5° × 0.5° (55 km)	0.05° × 0.05° (5 km)	0.5° × 0.5° (55 km)
Calculation area	Global 75°N – 75°S	Coastal Sea of Japan 50°N – 20°N, 120°E – 150°E	Global 75°N – 75°S
Grids	720 × 301	601 × 601	720 × 301
Spectral components	900 (25 frequencies and 36 directions) Frequency: 0.0375 – 0.3 Hz; logarithmically divided direction: 10° intervals		
Forecast cycle	4 times a day (every 6 hours)		Twice a day (every 12 hours)
Forecast length			264 hours

(12 UTC) (00/06/18 UTC)	264 hours 132 hours	132 hours 132 hours	
Forecast time interval	Every 3 hours	Every 3 hours	Every 6 hours
Time step	Advection term: 10 minutes Source term: 30 minutes	Advection term: 1 minute Source term: 3 minutes	Advection term: 10 minutes Source term: 30 minutes
Assimilation	Wave height analyzed using the Objective Wave Analysis System Initial conditions modified using analysis wave height		
Surface forcing	Global Spectral Model (GSM) (20 km grid) Winds inside typhoons modified using ideal gradient wind values (– 72 hours)		Global Ensemble Prediction System (GEPS) 27 members
Lateral boundary	Sea ice: analysis area regarded as land	Sea ice: analysis area regarded as land GWM prediction used for boundary spectra	Sea ice: analysis area regarded as land
Shallow-water effects	Refraction and bottom friction		
Product	Significant wave height, wave period and mean wave direction Wave components (windsea and two swells) also calculated		

Table 4.5.2.1 (2)-2 Shallow-water wave model specifications

Model name	Shallow-water Wave Model		
Model type	Spectral model (third-generation wave model)		
Grid interval	1' × 1' (1.7 km)		
Spectral components	1,260 (35 frequencies from 0.0418 to 1.1 Hz and 36 directions)		
Grid form	Equal latitude-longitude grid on spherical coordinates		
Areas	Domain name	Grid size	Integration domain
	Tokyo Bay	37 × 43	35.05°N – 35.75°N 139.55°E – 140.15°E
	Ise Bay	61 × 43	34.35°N – 35.05°N 136.45°E – 137.45°E
	Harima-Nada Osaka Bay	79 × 49	34.05°N – 34.85°N 134.15°E – 135.45°E
	Ariake Sea Shiranui Sea	43 × 73	32.05°N – 33.25°N 130.05°E – 130.75°E
	Off Niigata	55 × 37	37.80°N – 38.40°N 138.35°E – 139.25°E
	Sendai Bay	37 × 43	37.75°N – 38.45°N 140.90°E – 141.50°E
	Off Tomakomai	121 × 43	42.00°N – 42.70°N 141.00°E – 143.00°E
	Suo-Nada Iyo-Nada Aki-Nada	109 × 67	33.30°N – 34.40°N 131.00°E – 132.80°E
	Hiuchi-Nada	103 × 73	33.60°N – 34.80°N 132.60°E – 134.30°E
	Off Shimane	67 × 31	35.25°N – 35.75°N 132.55°E – 133.65°E
	Ishikari Bay	49 × 43	43.10°N – 43.80°N 140.70°E – 141.50°E
	Off Ishikawa	49 × 67	36.20°N – 37.30°N 136.00°E – 136.80°E

	Off Nemuro	85 × 49	43.20°N – 44.00°N 145.00°E – 146.40°E
	Off Miyazaki	31 × 73	31.50°N – 32.70°N 131.30°E – 131.80°E
	Tsugaru Strait	61 × 67	40.75°N – 41.85°N 140.35°E – 141.35°E
	Off Ibaraki Off Boso	49 × 103	35.00°N – 36.70°N 140.20°E – 141.00°E
	Genkai-Nada	85 × 43	33.40°N – 34.10°N, 129.55°E – 130.95°E
Forecast cycle	4 times a day (every 6 hours) at initial times of 03, 09, 15 and 21 UTC		
Forecast length	39 hours		
Forecast step interval	Hourly		
Integration time step	Advection term: 1 minute Source term: 1 minute		
Assimilation	No (hindcast)		
Surface forcing	Meso-Scale Model (MSM)		
	Bogus gradient winds (for typhoons in the western North Pacific)		
Lateral boundary	Sea ice: analysis area regarded as land CWM prediction used for boundary spectra		
Shallow-water effects	Refraction and bottom friction		
Product	Significant wave height, wave period and mean wave direction		

Wave model products are adopted by various domestic users (such as governmental organizations and private weather companies) via the Japan Meteorological Business Support Center (JMBSC), whereas SWM products are only used within JMA and MLIT's Regional Development Bureaus. GWM products are available within JMA's WMO Information System for National Meteorological and Hydrological Services (NMHSs), and are also disseminated to several countries via GTS.

(3) Storm surge models

JMA operates two storm surge models. One is used to predict storm surges in coastal areas of Japan using sea-surface wind and pressure fields inferred by the MSM. In the case of tropical cyclones (TCs), storm surges for six scenarios are predicted in consideration of TC track forecast errors. In addition to the MSM, TC bogus data corresponding to five tracks (center, faster, slower and rightmost/leftmost of the TC track forecast) are used for each scenario. Data on astronomical tides are required for the prediction of storm tides (i.e., the sum of storm surges and astronomical tides). Astronomical tides are estimated using an ocean tide model and added linearly to storm surges. The model's specifications are given in Table 4.5.2.1 (3)-1.

Table 4.5.2.1 (3)-1 Storm surge model (Japan region) specifications

Basic equations	Two-dimensional shallow-water equations
Numerical technique	Explicit finite difference method
Integration domain	Coastal areas of Japan (117.4°E – 150.0°E, 20.0°N – 50.0°N)
Grid	Adaptive Mesh Refinement (AMR) method 45 seconds (longitude gradually doubling to 12 minutes toward offshore areas) × 30 seconds (latitude gradually doubling to 8 minutes toward offshore areas)

Boundary conditions	Modified radiation condition at open boundaries and zero normal flows at coastal boundaries
Forecast time	39 hours
Forcing data	Meso-Scale Model (MSM)
	Bogus data for TCs around Japan
Astronomical tides	Ocean tide model (Egbert and Erofeeva, 2002) and data assimilation of harmonic constants at tide stations using the ensemble transform Kalman filter (ETKF)

As part of JMA's contribution to the Storm Surge Watch Scheme (a WMO framework supporting member countries in the issuance of storm surge warnings), the Agency developed a storm surge model for the Asian region in 2010 in collaboration with Typhoon Committee Members who provided tidal observation and sea bathymetry data. The model uses the GSM for meteorological forcing. For TCs, in addition to the GSM and TC bogus, multi-scenario predictions are calculated for five selected scenarios from GEPS data. The resulting storm surge prediction information is provided to Typhoon Committee Members via JMA's Numerical Typhoon Prediction website. The model's specifications are given in Table 4.5.2.1 (3)-2.

Table 4.5.2.1 (3)-2 Storm surge model (Asian region) specifications

Basic equations	Two-dimensional linear shallow-water equations
Numerical technique	Explicit finite difference method
Integration domain	Coastal areas of Asia (95.0°E – 160.0°E, 0.0°N – 46.0°N)
Grid	2 minutes × 2 minutes
Boundary conditions	Modified radiation condition at open boundaries and zero normal flows at coastal boundaries
Forecast time	72 hours
Forcing data	Global Spectral Model (GSM), Global EPS (GEPS)
	Bogus data for TCs (center)
Astronomical tides	Not included

(4) Ocean data assimilation system for the North Pacific Ocean

A 3D-Var ocean data assimilation system for the North Pacific is operated to represent ocean characteristics such as the Kuroshio path variation in the mid/high latitudes of the North Pacific with the specifications shown in Table 4.5.2.1 (4)-1. Data on ocean currents and several layers of subsurface water temperatures (products of this system) are available on the NEAR-GOOS Regional Real Time Database (https://www.data.jma.go.jp/goos/data/database.html).

Table 4.5.2.1 (4)-1 Specifications of the 3D-Var ocean data assimilation system for the North Pacific Ocean

Basic equations	Primitive equations with free surface
Independent variables	Lat-lon coordinates and σ-z hybrid vertical coordinates
Dependent variables	Zonal/meridional velocities, temperature, salinity and sea surface height
Analysis variables	Sea-surface/subsurface temperature and salinity
Numerical technique	Finite difference both in the horizontal and in the vertical

Grid size	(1) Western North Pacific model 0.1° longitude × 0.1° latitude in the seas off Japan, decreasing to 0.166° toward the northern and eastern boundaries (2) North Pacific model 0.5° longitude × 0.5° latitude
Vertical levels	54
Integration domain	(1) Western North Pacific model From 15°N to 65°N between 115°E and 160°W (2) North Pacific model From 15°S to 65°N between 100°E and 75°W
Forcing data	Heat, water and momentum fluxes from the Japanese 55-year Reanalysis (JRA-55) and from the control run of Global Ensemble Prediction System (GEPS)
Assimilation scheme	3D-Var with 5-day windows
Observational data (as of 31 December 2020)	Sea-surface and subsurface temperature/salinity, sea surface height (Jason-3, Cryosat-2, Saral), sea ice concentration
Operational runs	10-day assimilation and 30-day prediction are implemented every day

For enhanced marine information services, JMA's new MOVE/MRI.COM-JPN coastal ocean analysis/prediction system was implemented in October 2020 with a nested set of ocean models (global (GLB), North Pacific (NP), and Japanese coast (JPN)) and a 4D-Var ocean data assimilation system. The JPN model covers the whole of the Japanese coast with grid spacing of approximately 2 km, and represents oceanographic sub-meso scale events in coastal seas around the country. For details, see Sakamoto et al. (2019) and Hirose et al. (2019).

Table 4.5.2.1 (4)-2 MOVE/MRI.COM-JPN specifications

Basic equations	Primitive with free surface conditions
Independent variables	Lat-lon horizontal coordinates and z* vertical coordinates
Dependent variables	Zonal/meridional velocities, temperature, salinity, sea surface height and sea ice parameters
Analysis variables	Sea-surface/subsurface temperature and salinity
Numerical technique	Finite difference horizontal and vertical
Grid size	GLB: 1° longitude × 0.5° latitude NP: 1/11° longitude × 1/10° latitude JPN: 1/33° longitude × 1/50° latitude
Vertical levels	60
Integration domain	GLB: global NP: 15°S – 63°N, 99°E – 75°W JPN: 20° – 52°N, 117° – 160°E
Forcing data	Heat and water fluxes; surface wind, pressure, temperature, and humidity from JRA-55, GSM, and GEPS control run
Assimilation scheme	4D-Var with 10-day assimilation window
Observational data (as of 31 December 2020)	Sea-surface and subsurface temperature/salinity, sea surface height (Jason-3, Cryosat-2, Saral), sea ice concentration
Operational runs	Global model and North Pacific model: 30-day prediction Japan area model: 11-day prediction

(5) Sea-ice forecasting model

JMA issues information on the state of sea ice in the seas off Japan. A numerical sea-ice model has

been run to predict sea ice distribution and thickness in the seas off Hokkaido (mainly in the southern part of the Sea of Okhotsk) twice a week in winter since December 1990 (see Table 4.5.2.1 (5)-1).

Table 4.5.2.1 (5)-1 Numerical sea-ice prediction model specifications

Dynamical processes	Viscous-plastic model (MMD/JMA 1993) – considering wind and seawater stress on sea ice, Coriolis force, force from the sea surface gradient and internal force
Physical processes	Heat exchange between sea ice, the atmosphere and seawater
Dependent variables	Concentration and thickness
Grid size and time step	12.5 km and 6 hours
Integration domain	Seas around Hokkaido
Initial time and forecast time	168 hours from 00 UTC (twice a week)
Initial condition	Concentration analysis derived from Himawari-8/9, NOAA and Metop satellite imagery; thickness estimated by hindcasting

Grid-point values of the numerical sea-ice model are disseminated to domestic users. Sea ice conditions for the coming seven days as predicted by the model are broadcast by radio facsimile (JMH) twice a week.

(6) Marine pollution transport model

JMA operates the numerical marine-pollution transport model in the event of marine-pollution accidents. Its specifications are shown in Table 4.5.2.1 (6)-1. The ocean currents used for the model's input data are derived from the results of MOVE/MRI.COM-JPN (4.5.2.1 (4)).

Table 4.5.2.1 (6)-1 Marine pollution transport model specifications

Area	Western North Pacific
Grid size	2 – 30 km (variable)
Model type	3-dimensional parcel model
Processes	Advection caused by ocean currents, sea surface winds and ocean waves Turbulent diffusion Chemical processes (evaporation, emulsification)

(7) Aeolian dust analysis and prediction system

JMA has operated a prediction model since January 2004 to forecast Aeolian dust distribution. The model was updated to a new version based on an Earth-system model (MRI-ESM1; Yukimoto et al., 2011; Yukimoto et al., 2012) for global climate change research in November 2014, and the horizontal resolution was enhanced from TL159 to TL479 in February 2017. The model consists of an atmospheric general circulation model (AGCM) called MRI-AGCM3 and a global aerosol model called MASINGAR mk-2, which are linked with a coupler library called Scup (Yoshimura and Yukimoto, 2008). The dust emission flux calculation method was updated to encompass the scheme of Tanaka

and Chiba (2005) in November 2014.

JMA began Aeolian dust distribution analysis in January 2020, with two-dimensional variation (2D-Var) data assimilation of aerosol optical depth (AOD) at 500 nm as per Yumimoto et al. (2017). AOD observation for aerosol data assimilation is based on the AHI sensor on the Himawari-8 geostationary satellite, with a retrieval algorithm developed by the JAXA Earth Observation Research Center (JAXA EORC) (Kikuchi et al., 2018; Yoshida et al., 2018). 2D-Var data assimilation is conducted daily at 06 UTC. The model's specifications are given in Table 4.5.2.1 (7)-1.

Table 4.5.2.1 (7)-1 Aeolian dust analysis and prediction system specifications

Basic equations	Eulerian model coupled with the Global Spectral Model
Numerical technique	3D semi-Lagrangian transport and dust emission calculation from surface meteorology
Integration domain	Global
Grid size	TL479 (0.375°)
Vertical levels	40 (surface – 0.4 hPa)
Initial time and forecast time	96 hours from 12 UTC (once a day)
Boundary conditions	Similar to those of the Global Spectral Model
Forcing data (nudging)	Global Analysis (GA) and Global Spectral Model (GSM) forecasts
	Sea surface temperature (MGDSST)
Data assimilation	2-dimensional variation (2D-Var)
Observational data for assimilation	Aerosol optical depth at 500 nm from AHI

(8) Ultraviolet (UV) index prediction system

JMA has operated a UV index prediction system since May 2005. The UV index is calculated using a chemical transport model (CTM) that predicts the global distribution of ozone and a radiative transfer model. In October 2014, the ozone chemistry model was updated to a new version of the chemistry-climate model (MRI-CCM2; Deushi and Shibata, 2011), which is part of MRI-ESM1, and its horizontal resolution was enhanced from T42 to T106. Nudging for total column ozone assimilation is implemented. (See Table 4.5.2.1 (8)-1 for model specifications)

The radiative transfer model (Aoki et al., 2002) calculates the UV index in the area from 122°E to 149°E and from 24°N to 46°N with a grid resolution of 0.25° × 0.20°. The Look-Up Table (LUT) method is adopted in consideration of the computational cost involved. The basic parameters of LUT are the solar zenith angle and total ozone predicted using the CTM. The clear sky UV index is corrected for distance from the sun to the earth, aerosols (climatology), altitude and surface albedo (climatology). The forecast UV index is corrected for categorized weather forecasts in addition to the above-mentioned factors. The specifications of the radiative transfer model for the UV index are given in Table 4.5.2.1 (8)-2.

Table 4.5.2.1 (8)-1 Specifications of the chemical transport model in the UV index prediction system

Basic equations	Eulerian model coupled with the Global Spectral Model
Numerical technique	3D semi-Lagrangian transport and chemical reaction
Integration domain	Global

Grid size	T106 (1.125°)
Vertical levels	64 (surface – 0.01 hPa)
Initial time and forecast time	120 hours from 12 UTC (once a day)
Boundary conditions	Similar to those of the Global Spectral Model
Forcing data (nudging)	Global analysis (GA) and Global Spectral Model (GSM) forecasts
Observational data	Total column ozone from OMPS/NOAA

Table 4.5.2.1 (8)-2 Specifications of the radiative transfer model in the UV index prediction system

Basic equations	Radiative transfer equations for multiple scattering and absorption by atmospheric molecules and aerosols
Numerical technique	Doubling and adding method
Spectral region and resolution	280 – 400 nm and 0.5 nm

(9) Regional chemical transport model for photochemical oxidants

JMA provides prefectural governments with photochemical smog bulletins as a basis for related advisories. The bulletins are produced by numerical model prediction of tropospheric photochemical oxidant distribution and a statistical guidance derived from model outputs associated with past events.

Since March 2015, photochemical oxidant concentrations have been numerically predicted using a regional chemical transport model (NHM-Chem; Kajino et al., 2019), with 20-km spatial resolution driven by meteorological fields predicted using a non-hydrostatic atmospheric model (JMA-NHM). The related lateral and upper boundary conditions for chemical species are given by MRI-CCM2 as described in 4.5.2.1 (8).

Since March 2017, surface ozone concentration observation data have been assimilated in photochemical oxidant prediction. The specifications of the regional chemical transport model are given in Table 4.5.2.1 (9)-1.

Since March 2020, a nested model domain has been employed in finer-scale simulation for central Japan. In the nested 5-km-scale model (ASUCA-Chem), meteorological fields predicted using the new forecast model (ASUCA; Aranami et al., 2015) were used. The lateral and upper boundary conditions for chemical species are taken from NHM-Chem (20 km). The specifications of the nested model are given in Table 4.5.2.1 (9)-2. The NHM-Chem source code is available subject to a license agreement with the Japan Meteorological Agency. Further resources, including a user's manual and analysis tools, can be provided upon request to the Meteorological Research Institute.

Table 4.5.2.1 (9)-1 Specifications of the regional chemical transport model for photochemical oxidants

Model type	3-dimensional Eulerian chemical transport model
Area	East Asia

Grid size	20 km
Vertical layers	18 (surface – 10 km)
Forecast time	72 hours (initial time 12 UTC)
Emission inventories	REAS1.1, GFED3 and MEGAN2
Meteorological fields	JMA-NHM output constrained and initialized using Global Analysis (GA) and Global Spectral Model (GSM) forecasts
Observational data	Surface O_3 concentration of Atmospheric Environmental Regional Observation System (AEROS**)

** Available from https://soramame.env.go.jp/

Table 4.5.2.1 (9)-2 Specifications of the nested regional chemical transport model

Model type	3-dimensional Eulerian chemical transport model
Area	Central Japan (approx., 129 – 141°E, 31 – 38°N)
Grid size	5 km
Vertical layers	19 (surface – 10 km)
Forecast time	51 hours (initial time 12 UTC)
Emission inventories	EAGrid2010, GFED3 and MEGAN2
Meteorological fields	ASUCA output (MA)
Observational data	Surface O_3 concentration from the Atmospheric Environmental Regional Observation System (AEROS**)

(10) Mesoscale air pollution transport model

JMA also issues very-short-term photochemical smog bulletins on days when high oxidant concentration is expected. The bulletins provide an outlook for photochemical smog based on statistical guidance for oxidant concentration using data on weather elements and pollutant observation data as input. In addition to this statistical guidance, a mesoscale atmospheric transport model (Takano et al., 2007) is applied to very-short-range forecasting of oxidant concentrations with a grid interval of 10 km, with MSM output used to calculate the transport of highly concentrated pollutant masses in the air. Based on the oxidant forecast from the atmospheric transport model with an initial time of 03 UTC (noon in Japan), photochemical smog bulletins show hourly potential for afternoon smog in the northern part of the Kyushu region and the Kanto region, where the Tokyo metropolitan area is located.

(11) Regional Atmospheric Transport Model (RATM) for volcanic ash

JMA introduced the Volcanic Ash Fall Forecast (VAFF) based on the Regional Atmospheric Transport Model (RATM) in March 2008 (Shimbori et al., 2009) and updated it in spring 2015 (Hasegawa et al., 2015). Three types of forecasts are sequentially provided: VAFFs (Scheduled) are issued periodically based on an assumed eruption for active volcanoes, VAFFs (Preliminary) are brief forecasts issued within 5 — 10 minutes of an actual eruption, and VAFFs (Detailed) are more accurate forecasts issued within 20 — 30 minutes of an actual eruption. The updated VAFFs provide information on expected ash/lapilli fall areas and/or amounts based on the RATM with LFM or MSM outputs. The specifications of RATM are given in Table 4.5.2.1 (11)-1.

Table 4.5.2.1 (11)-1 Specifications of RATM for volcanic ash

Model type	Lagrangian description
Number of tracer particles	100,000 (Scheduled, Preliminary) 250,000 (Detailed)
Time step	1 minute (Preliminary) 3 minutes (Scheduled, Detailed)
Forecast time	18 hours from the time of assumed eruption (Scheduled) 1 hour from the time of eruption (Preliminary) 6 hours from the time of eruption (Detailed)
Initial condition	Eruption column based on observational reports including eruption time and plume height, and continuance of volcanic-ash emissions
Meteorological field	Local Forecast Model (LFM) or Meso-Scale Model (MSM)
Processes	3D advection, horizontal and vertical diffusion, volcanic-ash fallout, dry deposition and washout

(12) Global Atmospheric Transport Model (GATM) for volcanic ash

Since 1997, JMA has been providing information on volcanic ash clouds to airlines, civil aviation authorities and related organizations in its role as the Volcanic Ash Advisory Center (VAAC) Tokyo. JMA introduced the Global Atmospheric Transport Model (GATM) in December 2013 as an 18-hour prediction of areas where ash clouds are expected in the area of responsibility as a result of volcanic eruptions. The forecast is normally updated every six hours (00, 06, 12 and 18 UTC) for as long as ash clouds are identified in satellite imagery. The specifications of the GATM are given in Table 4.5.2.1 (12)-1.

Table 4.5.2.1 (12)-1 Specifications of GATM for volcanic ash

Model type	Lagrangian description
Number of tracer particles	40,000
Time step	10 minutes
Forecast coverage	18 hours from the time of satellite observation
Initial condition	Location of volcanic ash particles based on the area and maximum altitude of volcanic ash cloud observed by satellite
Meteorological field	Global Spectral Model (GSM)
Processes	3D advection, (horizontal and vertical diffusion,) volcanic-ash fallout, dry deposition and washout

4.5.2.2 Research performed in this field

(1) Storm surge model

A new storm surge model that solves governing equations using the finite volume method on an unstructured grid is currently being developed. The use of such a grid allows grid-size flexibility, which is expected to enable improvements in forecast accuracy and computational efficiency compared to current models. The new model will be incorporated into both storm surge prediction systems.

(2) Sea-ice forecasting model

JMA plans to replace the current sea ice model (see 4.5.2.1 (5)) with the sea ice model component included in MOVE/MRI.COM-JPN (see 4.5.2.1 (4)). Sea ice data from MOVE/MRI.COM-JPN are currently being verified for operational use.

(3) Aeolian dust analysis and prediction system

Previous aerosol reanalysis research has included a development version of the Aeolian dust forecasting model and 2D-Var data assimilation with the NRL-UND MODIS L3 AOT product (Yumimoto et al., 2017). The reanalysis products are available from the authors upon request. Other research on determining aerosol properties from satellite data combined with assimilated aerosol forecasting is conducted in conjunction with JAXA/EORC (Yoshida et al., 2021)

(4) UV index prediction system

The implementation of variational data assimilation for stratospheric ozone with the use of satellite data is in the research phase.

(5) Regional chemical transport model

A nudging technique for surface ozone data assimilation in the regional chemical transport model will also be nested for operational use. Research toward the implementation of 2D-Var data assimilation is ongoing toward improved prediction for photochemical oxidants and aerosols. An emission super-ensemble method was also proposed for better prediction of surface ozone concentration over Japan (Kajino et al., 2021). A paper describing ASUCA-Chem and detailing analysis of high ozone concentrations in July 2018 is in preparation.

(6) Volcanic ash concentration forecast

Despite the importance of volcanic ash concentration forecasting in the world of aviation, no method for such prediction has yet been developed. JMA is currently evaluating a forecast method involving calculation with weight coefficients for individual particles, based on the comparison of actual results with observation data for past eruptions.

(7) Improvement of initial conditions for volcanic ash forecasts

JMA is currently developing a method to improve data on the initial distribution of volcanic ash for numerical prediction using estimation of ash cloud thickness.

4.5.3 Specific products operationally available

(1) Storm surge prediction products

Time series representations of predicted storm tides/astronomical tides and forecast time on predicted highest tides for the coastal area in Japan are disseminated to local meteorological observatories. This information is used as a major basis for issuing storm surge advisories and warnings. For the area of responsibility of the RSMC Tokyo - Typhoon Center, horizontal maps and time-series charts of storm surge predictions are provided to Typhoon Committee members via JMA's Numerical Typhoon Prediction website.

(2) Ocean wave forecast charts

Products from the ocean wave models shown in Table 4.2.3-1 are provided via JMA's radio facsimile broadcast (JMH) service. In addition to basic wave information such as significant wave height and wave direction, information on rough sea areas, which may be challenging for navigation, has been included in Wave Forecast Charts since March 2017. The information indicates areas of crossing waves and rough waves against currents, which make seas complex, high and chaotic.

(3) Aeolian dust products operationally available

Predicted distributions of surface concentration and the total amount of Aeolian dust in eastern Asia are provided online (https://www.data.jma.go.jp/env/kosa/fcst/en/) once a day.

(4) UV index products operationally available

Distributions and time series representations of predicted UV index information are provided online (https://www.data.jma.go.jp/env/uvindex/en/) twice a day.

4.6 Extended-range forecasts (ERFs) (10 – 30 days)

4.6.1 Models

4.6.1.1 In operation

The Global EPS (GEPS) referred to in 4.2.5.1 seamlessly covers medium- to extended-range forecasting. The GEPS forecast range is extended from 11 to 18 days for initial times every day and to 34 days for initial times on Tuesday and Wednesday. JMA's 18-day forecasts support the issuance

of early warning information on extreme weather and two-week temperature forecast, and 34-day forecasts support one-month forecasting.

The specifications of the GEPS for forecasts longer than 11 days are shown in Table 4.6.1.1-1. The numerical prediction model applied for this system is a low-resolution version (TL479 up to 18 days and TL319 thereafter) of the GSM. The physical schemes and perturbation methods for forecasts longer than 11 days are shared with those for forecasts up to 11 days, while the prescription of sea ice and the combination of ensemble members are unique. Sea ice concentration for forecasts longer than 14 days is prescribed by adjusting the previous day's distribution so that initial sea ice extent anomalies in each hemisphere persist. In addition, because the ensemble size for each initial time is reduced from 27 to 13 for forecasts longer than 11 days due to limited computer resources, JMA adopts the Lagged Average Forecast (LAF) method composed of four 12-hour-interval forecasts for periods exceeding 11 days to ensure a significant ensemble member size and appropriate consideration of forecast uncertainty. Specifically, 50 members (13 at 00 and 12 UTC over the previous two days) are used for the issuance of early warning information on extreme weather on Thursday/Monday and one-month forecasts on Thursday.

Table 4.6.1.1-1 Global EPS specifications for forecasts longer than 11 days

Atmospheric model	GSM2003
Integration domain	Global
Horizontal resolution	Spectral triangular 479 (TL479), reduced Gaussian grid system, roughly equivalent to 0.375 × 0.375° (40 km) in latitude and longitude for forecasts up to 18 days Spectral triangular 319 (TL319), reduced Gaussian grid system, roughly equivalent to 0.5625 × 0.5625° (55 km) in latitude and longitude for forecasts longer than 18 days
Vertical levels (model top)	100 stretched sigma pressure hybrid levels (0.01 hPa)
Forecast time	18 days for initial times every day 34 days for initial times on Tuesday and Wednesday
Ensemble size	50 members (13 at 00 and 12 UTC over the previous two days)

4.6.1.2 Reanalysis project

In March 2013, JMA completed the second Japanese global reanalysis, known formally as JRA-55 (Kobayashi et al., 2015) and informally as JRA Go! Go! (as “go” is the Japanese word for “five”), to provide a comprehensive atmospheric dataset suitable for the study of climate change and multi-decadal variability. The data cover a period of 55 years extending back to 1958 when regular radiosonde observations became operational on a global basis. The data assimilation system for JRA-55 is based on the TL319 version of JMA’s operational data assimilation system as of December 2009, which has been extensively improved since the JRA-25 dataset was produced (Onogi et al., 2007). JRA-55 is the first global atmospheric reanalysis in which four-dimensional variational assimilation (4D-Var) was applied to the last half century including the pre-satellite era. Its production also involved the use of numerous newly available and improved past observations. The resulting

reanalysis products are considerably better than those based on the JRA-25 dataset. Two major problems with JRA-25 were a lower-stratosphere cold bias, which has now been reduced, and a dry bias in the Amazon basin, which has been mitigated. The temporal consistency of temperature analysis has also been considerably improved. JMA continues the production of JRA-55 dataset on a near-real-time basis with the data assimilation system used for this dataset.

To further improve the quality of re-analysis data and contribute to advancing climate services and applications, JMA is currently conducting a third Japanese global atmospheric re-analysis (the Japanese Reanalysis for Three Quarters of a Century (JRA-3Q)) covering the period from the late 1940s to the present based on the TL479 resolution version of the Agency's operational data assimilation system as of December 2018, which has been extensively improved since the JRA-55 re-analysis. In JMA's Global Spectral Model, for example, biases of radiation budget, surface sensible/latent heat fluxes and precipitation have been significantly reduced due to extensive improvement of parameterizations for physical processes. A boundary condition over the ocean for the mid-1980s onward has also been replaced with satellite-based high-resolution (0.25-deg) SST data (MGDSST) to improve the representation of atmospheric processes around western boundary currents and associated SST fronts. JMA plans to start near-real-time production of the JRA-3Q dataset in 2021 as with JRA-55.

4.6.2 Operationally available NWP model and EPS ERF products

A model systematic bias was estimated as an average forecast error calculated from hindcast experiments for the years from 1981 to 2010. Bias is removed from geopotential height, sea level pressure and temperature in advance to produce ensemble forecast products such as ensemble means and spreads.

Gridded data products for one-month forecast are provided via the Tokyo Climate Center (TCC) website (https://ds.data.jma.go.jp/tcc/tcc/index.html). Details of these products are shown in Table 4.6.2-1, and map products provided via the TCC are shown in Table 4.6.2-2.

Table 4.6.2-1 Gridded data products (GRIB2) for one-month forecasts provided via the TCC website

Details		Level (hPa)	Area	Base time & forecast times
Ensemble mean value of forecast members	Sea level pressure* and its anomaly	-	Global 2.5° × 2.5° and 1.25° ×	Base time: 00 UTC of Wednesday Forecast time: 2, 3, 4…,31,32 days from base time
	Daily mean precipitation and its anomaly	-		
	Temperature* and its anomaly	Surf, 850, 700		
	Relative humidity	850		

	Geopotential height* and its anomaly	500, 100	1.25°	
	Wind (u, v)	850, 200		
	Stream function and its anomaly	850, 200		
	Velocity potential and its anomaly	200		
Individual ensemble members	Sea level pressure*	-		Base time: 00 UTC of Tuesday and Wednesday Forecast time: 0, 1, 2, ..., 32, 33 days from base time
	Daily mean precipitation	-		
	Temperature*	Surf, 1000, 850, 700, 500, 300, 200, 100		
	Relative humidity	1000, 850, 700, 500, 300		
	Geopotential height*	1000, 850, 700, 500, 300, 200, 100		
	Wind (u,v)	1000, 850, 700, 500, 300, 200, 100		
	Stream function	850, 200		
	Velocity potential	200		

* Geopotential height, sea level pressure and temperature are calibrated by subtracting the systematic error from the direct model output.

Table 4.6.2-2 Map products for one-month forecasts provided via the TCC website

	Forecast time	Parameter
Ensemble mean	Averages of days 3 – 9, 10 – 16, 17 – 30, 3 – 30	Geopotential height at 500 hPa and its anomaly Temperature at 850 hPa and its anomaly Sea level pressure and its anomaly Stream function at 200 hPa and its anomaly Stream function at 850 hPa and its anomaly Velocity potential at 200 hPa and its anomaly Precipitation and its anomaly Temperature at 2 m and its anomaly Sea surface temperature (prescribed)

4.7 Long range forecasts (LRF) (30 days up to two years)

4.7.1 Models

4.7.1.1 In operation

JMA operates its Seasonal Ensemble Prediction System (Seasonal EPS; JMA/MRI-CPS2) using a coupled atmosphere-ocean model for three-month, warm/cold season and El Niño outlooks. The current system was upgraded in June 2015. The 51-member ensemble is used for the three-month forecast issued every month and for the warm/cold season forecasts issued five times a year (in February, March, April, September and October). The El Niño outlook is also issued based on the same model results.

The JMA/MRI-CPS2 was developed by JMA and the Meteorological Research Institute (MRI). Its specifications are shown in Table 4.7.1.1-1. Atmospheric and land surface initial conditions are taken

from JRA-55 data (Kobayashi et al., 2015; 4.6.1.2), while oceanic and sea ice initial conditions are taken from MOVE/MRI-COM-G2 (4.5.1.1 (1)). The EPS adopts a combination of the LAF method and the initial perturbation method described below. Thirteen-member ensemble predictions are made every five days, and atmospheric initial perturbations for each initial date are obtained using the BGM method. Oceanic initial perturbations are obtained with MOVE/MRI.COM-G2 forced by the surface heat and momentum fluxes of atmospheric initial perturbation fields using the BGM method.

Table 4.7.1.1-1 Seasonal EPS specifications

1. System

System	JMA/MRI-CPS2	JMA/MRI-CPS3
Operation start	June 2015	January 2022 (TBD)

2. Configuration

Atmospheric model	Version	GSM1011C	GSM2003C
	Resolution	Global TL159 reduced Gaussian grid (– 110 km)	Global TL319 reduced Gaussian grid (– 55 km)
	Vertical levels (model top)	60 (0.1 hPa)	100 (0.01 hPa)
Oceanic model	Version	MRI.COM v3.2	MRI.COM v4.6
	Horizontal resolution	1 (longitude) × 0.3 – 0.5° (latitude)	0.25 (longitude) × 0.25° (latitude)
	Vertical levels	52 with bottom boundary layer	60 levels
Forecast period		7 months	
Forecast frequency		13 ensemble members every 5 days	5 ensemble members every day
Initial conditions	Atmosphere	JRA-55	JRA-3Q (hindcasts + forecasts) Global Analysis (GA; forecasts only)
	Land surface	JRA-55	Offline model runs forced using JRA-3Q and GA
	Ocean	MOVE/MRI.COM-G2 (3DVAR)	MOVE/MRI.COM-G3 (low-res. 4DVAR + high-res downscaling)
	Sea ice		MOVE/MRI.COM-G3 (3DVAR)
Ensemble generation	Initial condition perturbation	Breeding of growing mode (BGM) Lagged average forecast (LAF)	BGM for the atmosphere Ocean perturbations calculated using 4DVAR minimization history LAF method
	Model perturbation (atmosphere)	Stochastic physics scheme	
Hindcasts	Period	Two initial dates per month for the period from 1979 to 2014	Two initial dates per month for the period from 1991 to 2020

	Ensemble size	Five for each initial date

4.7.1.2 Research performed in this field

JMA plans to upgrade the Seasonal EPS in January 2022. The new JMA/MRI-CPS3 system will incorporate a wide range of research results achieved by JMA and MRI (Table 4.7.1.1-1). The atmospheric model is from GSM2003, with additional improvements such as cloud and cumulus convection schemes (referred to here as GSM2003C). Atmospheric conditions are initialized with JRA-3Q for reforecasts, and Global Analysis (GA) allowing faster atmospheric updates is also used in operation to broaden scope toward sub-seasonal forecasts. Land is initialized separately from this analysis due to inconsistencies in lake/land treatment in the model, including GSM2003C's newly-developed lake scheme requiring initialization. To this end, the model's off-line land surface simulation will be used. Ocean and sea ice initial conditions are taken from MOVE/MRI.COM-G3 (see 4.5.1.1 (1)), but with downscaling into eddy-permitting ocean resolution (0.25 by 0.25° in longitude and latitude). The EPS will feature a combination of LAF and initial perturbation as with the previous system. Five-member ensemble predictions are made every day, and atmospheric initial perturbations for each initial date are obtained using the BGM. Ocean initial perturbations are calculated using 4DVAR minimization history to approximate the day's analysis error covariance.

4.7.2 Operationally available EPS LRF products

JMA provides gridded data and map products for three-month forecasts every month. Warm-season (June-July-August; JJA) forecasts are issued in February, March and April, and cold-season (December-January-February; DJF) forecasts are issued in September and October.

A model systematic bias was estimated for use as an average forecast error calculated from hindcast experiments for the 30 years from 1981 to 2010. Bias is removed from geopotential height, sea level pressure, temperature and sea surface temperature in advance to produce ensemble forecast products such as ensemble means and spreads.

The following model output products for three-month, warm/cold-season (Tables 4.7.2-1, 4.7.2-2 and 4.7.2-3) and six-month (Tables 4.7.2-1) forecasts are provided via the Tokyo Climate Center (TCC) website (https://ds.data.jma.go.jp/tcc/tcc/index.html).

Table 4.7.2-1 Gridded data products (GRIB2) for three-month, warm/cold-season and six-month forecasts provided via the TCC website

Details		Level (hPa)	Area	Base time & forecast time
Ensemble mean, its anomaly, and spread	Sea level pressure*, its anomaly and spread	-	Global	Base time: 00 UTC around the 15th of each month (three-month and
	Daily mean precipitation, its anomaly and spread	-		

(standard deviation) values of forecast members	Sea surface temperature* and its anomaly	-	2.5˚ × 2.5˚	warm/cold season forecasts) and 00UTC every 5 days (six-month forecasts) Forecast times: One- and three-month averages for targeted terms
	Temperature*, its anomaly and spread	Surf, 850		
	Geopotential height*, its anomaly and spread	500		
	Wind (u, v), its anomaly and spread	850, 200		
Individual ensemble members	Sea level pressure* and its anomaly	-		Base time: 00 UTC on each initial date of prediction (every 5 days) Forecast times: One-month averages for targeted terms
	Daily mean precipitation and its anomaly	-		
	Sea surface temperature* and its anomaly	-		
	Temperature* and its anomaly	Surf, 850, 500, 200		
	Relative humidity and its anomaly	850		
	Specific humidity and its anomaly (only for three-month and warm/cold season forecasts)	850		
	Geopotential height* and its anomaly	850, 500, 300, 200, 100		
	Wind (u, v) and its anomaly	850, 500, 200		

* Geopotential height, sea level pressure, temperature and sea surface temperature are calibrated by subtracting the systematic error from the direct model output.

Table 4.7.2-2 Map products for three-month and warm/cold-season forecasts provided via the TCC website
<https://ds.data.jma.go.jp/tcc/tcc/products/model/map/4mE/index.html>

	Forecast time	Parameter
Ensemble mean, its anomaly and spread	Three-month forecast: Averages of first month, second month, third month, and three months Warm/cold season forecast: Averages of three months (JJA or DJF)	Geopotential height at 500 hPa, related anomaly and spread Temperature at 850 hPa, its anomaly and spread Sea level pressure, its anomaly and spread Stream function at 200 hPa, its anomaly and spread Stream function at 850 hPa, its anomaly and spread Wind (u, v) anomaly at 850 hPa Velocity potential at 200 hPa, its anomaly and spread Precipitation, its anomaly and spread Temperature at 2 m, its anomaly and spread Sea surface temperature and its anomaly

Table 4.7.2-3 SST Index Time Series
<https://ds.data.jma.go.jp/tcc/tcc/products/model/indices/3-mon/indices1/shisu_forecast.php>

Index	Description	Coordinates
NINO.1+2	Region off coasts of Peru and Chile	90°W – 80°W, 10°S – 0°
NINO.3	Eastern/Central Tropical Pacific	150°W – 90°W, 5°S – 5°N
NINO3.4	Central Tropical Pacific	170°W – 120°W, 5°S – 5°N
NINO.4	Western/Central Tropical Pacific	160°E – 150°W, 5°S – 5°N
NINO.WEST	Western Tropical Pacific	130°E – 150°W, 0°– 15°N
TNA	Tropical North Atlantic	55°W – 15°W, 5°N – 25°N
TSA	Tropical South Atlantic	30°W – 10°E, 20°S – 0°

TAD	Tropical Atlantic Dipole	TNA – TSA
IOBW	Indian Ocean Basin-Wide	40°E – 100°E, 20°S – 20°N
WTIO	Western Tropical Indian Ocean	50°E – 70°E, 10°S – 10°N
SETIO	Southeastern Tropical Indian Ocean	90°E – 110°E, 10°S – 0°
IOD	Indian Ocean Dipole	WTIO – SETIO

5. Verification of prognostic products

5.1 Annual verification summary

5.1.1 NWP prognostic products

Prognostic products are objectively verified against analysis and radiosonde observations according to the WMO/CBS standardized procedures for verification of deterministic NWP products as defined in the Manual on the Global Data-processing and Forecasting System.

The results of monthly verification for 2020 are presented in Tables 5.1.1-1 – 5.1.1-20. All verification scores are only for prediction from 1200 UTC initials, and are computed using procedures approved at the 16th WMO Congress in 2011.

Table 5.1.1-1 Root mean square errors of geopotential height at 500 hPa against analysis (m)

Northern Hemisphere (20–90˚N)

Hours	Jan	Feb	Mar	Apr	May	Jun	Jul	Aug	Sep	Oct	Nov	Dec	Annual
24	7.6	7.8	7.2	6.7	6.1	5.9	5.6	5.6	6.0	6.4	6.8	7.1	6.6
72	24.1	23.3	23.7	22.5	21.2	19.6	17.4	17.0	18.2	20.5	21.4	22.5	21.1
120	48.8	47.2	50.3	49.1	44.4	40.8	37.5	33.9	36.2	43.2	44.0	43.9	43.6

Table 5.1.1-2 Root mean square errors of geopotential height at 500 hPa against analysis (m)

Southern Hemisphere (20–90˚S)

Hours	Jan	Feb	Mar	Apr	May	Jun	Jul	Aug	Sep	Oct	Nov	Dec	Annual
24	7.1	7.1	7.6	8.0	8.4	8.5	8.9	8.7	8.5	8.0	7.2	6.7	7.9
72	22.2	22.0	24.9	28.9	27.2	28.1	31.1	30.1	28.8	27.5	23.1	21.1	26.5
120	44.4	45.0	51.7	61.3	56.6	57.4	60.5	59.0	59.3	50.3	48.4	44.2	53.6

Table 5.1.1-3 Root mean square errors of geopotential height at 500 hPa against observations (m)

North America

Hours	Jan	Feb	Mar	Apr	May	Jun	Jul	Aug	Sep	Oct	Nov	Dec	Annual
24	11.6	11.6	10.6	10.2	9.8	9.0	8.1	8.4	9.3	10.2	10.6	11.8	10.2
72	30.1	27.5	23.6	21.6	23.4	18.3	13.9	14.2	21.5	24.6	25.0	31.4	23.5
120	56.4	52.9	49.4	44.4	41.9	37.3	29.1	25.0	38.1	43.2	47.6	60.2	44.9
ob. num.	86	86	86	86	87	86	86	84	83	83	84	84	

Table 5.1.1-4 Root mean square errors of geopotential height at 500 hPa against observations (m)

Europe/North Africa

Hours	Jan	Feb	Mar	Apr	May	Jun	Jul	Aug	Sep	Oct	Nov	Dec	Annual
24	15.2	15.1	11.9	9.9	9.7	9.6	9.0	8.8	9.9	11.7	12.5	14.0	11.7
72	29.3	27.9	27.4	23.2	22.4	24.7	18.4	16.8	19.9	24.4	22.1	21.8	23.4
120	61.4	57.5	54.4	51.8	48.8	48.3	35.9	32.6	44.0	53.1	52.2	44.4	49.3
ob. num.	51	50	51	55	53	53	52	48	48	48	47	46	

Table 5.1.1-5 Root mean square errors of geopotential height at 500 hPa against observations (m)

Asia

Hours	Jan	Feb	Mar	Apr	May	Jun	Jul	Aug	Sep	Oct	Nov	Dec	Annual
24	12.4	11.7	12.4	11.6	11.4	10.0	10.4	9.4	9.7	10.5	11.5	12.2	11.1
72	22.1	21.4	22.2	22.9	20.1	18.8	18.6	16.4	16.9	17.7	18.8	19.3	19.7
120	36.1	38.4	35.5	42.6	38.4	29.2	30.4	26.5	28.9	32.0	35.8	38.2	34.6
ob. num.	112	114	115	112	113	114	114	114	113	116	115	114	

Table 5.1.1-6 Root mean square errors of geopotential height at 500 hPa against observations (m)

Australia/New Zealand

Hours	Jan	Feb	Mar	Apr	May	Jun	Jul	Aug	Sep	Oct	Nov	Dec	Annual
24	15.4	15.1	14.6	15.4	14.5	14.2	13.6	13.2	11.8	11.0	11.8	12.2	13.7
72	21.5	18.0	22.6	26.5	22.2	24.3	25.8	22.7	25.0	18.8	19.2	18.8	22.3
120	36.9	28.9	37.3	43.3	46.3	42.0	43.8	45.5	40.2	35.8	37.7	35.6	39.8
ob. num.	14	14	14	13	13	13	13	13	13	13	13	13	

Table 5.1.1-7 Root mean square errors of geopotential height at 500 hPa against observations (m)

Northern Hemisphere (20–90˚N)

Hours	Jan	Feb	Mar	Apr	May	Jun	Jul	Aug	Sep	Oct	Nov	Dec	Annual
24	12.9	12.8	12.4	11.4	11.1	10.2	10.2	10.0	10.4	11.0	11.7	12.5	11.4
72	26.7	25.7	25.0	23.9	22.9	20.5	18.2	17.8	19.6	22.1	23.0	24.6	22.7
120	49.9	49.2	48.3	49.3	44.2	38.8	34.9	32.4	36.6	42.6	44.9	47.0	43.5
ob. num.	352	354	356	359	362	362	359	355	352	355	353	351	

Table 5.1.1-8 Root mean square errors of geopotential height at 500 hPa against observations (m)

Southern Hemisphere (20–90˚S)

Hours	Jan	Feb	Mar	Apr	May	Jun	Jul	Aug	Sep	Oct	Nov	Dec	Annual
24	11.5	11.1	10.9	12.2	12.6	12.7	12.4	12.9	11.9	11.3	10.8	11.1	11.8
72	20.2	17.6	19.4	24.5	24.2	25.2	28.4	27.0	24.5	24.3	19.7	19.6	23.2
120	34.4	30.4	36.8	45.4	49.9	49.0	49.8	50.9	45.6	42.7	38.8	36.5	43.1
ob. num.	44	42	39	37	33	34	35	38	39	41	43	44	

Table 5.1.1-9 Root mean square of vector wind errors at 250 hPa against analysis (m/s)

Northern Hemisphere (20–90˚N)

Hours	Jan	Feb	Mar	Apr	May	Jun	Jul	Aug	Sep	Oct	Nov	Dec	Annual
24	3.5	3.4	3.5	3.6	3.5	3.6	3.5	3.5	3.4	3.2	3.3	3.3	3.4
72	7.6	7.7	7.8	7.9	8.1	8.3	8.2	7.8	7.9	7.7	7.6	7.7	7.9

120	13.0	12.7	13.2	13.2	13.2	13.4	13.4	12.3	13.0	13.4	13.0	12.4	13.0

Table 5.1.1-10 Root mean square of vector wind errors at 250 hPa against analysis (m/s)

Southern Hemisphere (20–90˚S)

Hours	Jan	Feb	Mar	Apr	May	Jun	Jul	Aug	Sep	Oct	Nov	Dec	Annual
24	3.3	3.3	3.4	3.5	3.6	3.4	3.5	3.4	3.4	3.4	3.4	3.2	3.4
72	7.9	7.7	8.1	8.7	8.3	8.2	8.6	8.1	8.2	8.2	7.9	7.6	8.1
120	13.0	13.0	14.0	15.0	14.1	13.8	14.1	13.5	13.8	13.6	13.3	13.1	13.7

Table 5.1.1-11 Root mean square of vector wind errors at 250 hPa against observations (m/s)

North America

Hours	Jan	Feb	Mar	Apr	May	Jun	Jul	Aug	Sep	Oct	Nov	Dec	Annual
24	5.5	5.9	5.8	5.7	6.0	6.1	5.7	5.7	5.3	5.4	5.3	6.0	5.7
72	9.9	9.5	9.7	9.0	10.2	10.1	9.0	8.8	9.7	9.8	9.6	11.9	9.8
120	16.1	14.9	15.6	14.2	14.4	15.2	13.4	12.3	14.8	15.0	16.0	18.6	15.1
ob. num.	87	88	87	87	89	88	88	87	85	86	87	86	

Table 5.1.1-12 Root mean square of vector wind errors at 250 hPa against observations (m/s)

Europe/North Africa

Hours	Jan	Feb	Mar	Apr	May	Jun	Jul	Aug	Sep	Oct	Nov	Dec	Annual
24	4.9	5.5	4.6	4.8	5.1	5.2	4.7	5.1	5.3	5.6	4.6	5.1	5.0
72	9.6	10.2	8.0	9.0	9.7	10.4	8.9	8.8	9.7	10.3	8.4	8.5	9.3
120	18.0	17.1	14.0	14.6	15.6	16.9	15.0	14.3	16.4	17.2	15.9	14.1	15.8
ob. num.	54	53	54	58	57	56	55	51	50	49	50	48	

Table 5.1.1-13 Root mean square of vector wind errors at 250 hPa against observations (m/s)

Asia

Hours	Jan	Feb	Mar	Apr	May	Jun	Jul	Aug	Sep	Oct	Nov	Dec	Annual
24	5.0	4.9	5.7	6.0	6.6	6.5	6.6	5.8	5.5	4.2	4.3	4.2	5.5
72	7.5	8.0	8.6	9.6	10.3	10.4	10.5	9.3	8.6	6.6	6.7	6.5	8.7
120	10.6	11.0	11.1	13.2	14.8	13.5	14.6	12.4	12.1	10.1	11.1	9.9	12.1
ob. num.	132	137	135	134	135	135	135	136	137	138	137	137	

Table 5.1.1-14 Root mean square of vector wind errors at 250 hPa against observations (m/s)

Australia/New Zealand

Hours	Jan	Feb	Mar	Apr	May	Jun	Jul	Aug	Sep	Oct	Nov	Dec	Annual
24	5.5	5.2	5.7	5.8	5.6	5.0	5.3	5.2	5.3	5.2	6.0	6.1	5.5
72	8.2	7.4	8.9	9.7	8.2	7.3	8.3	7.6	8.8	7.9	9.4	8.9	8.4
120	12.1	11.0	13.0	15.1	13.6	10.5	13.8	11.3	11.7	11.2	13.7	13.6	12.6
ob. num.	15	15	14	14	13	13	13	13	14	14	15	15	

Table 5.1.1-15 Root mean square of vector wind errors at 250 hPa against observations (m/s)

Northern Hemisphere (20–90˚N)

Hours	Jan	Feb	Mar	Apr	May	Jun	Jul	Aug	Sep	Oct	Nov	Dec	Annual
24	4.9	5.1	5.3	5.4	5.7	5.7	5.7	5.4	5.2	4.7	4.6	4.7	5.2
72	8.5	8.6	8.5	8.9	9.7	9.8	9.5	9.0	8.9	8.3	8.0	8.6	8.9

120	13.8	13.3	13.0	13.8	14.4	14.3	14.3	13.1	13.7	13.3	13.4	13.3	13.7
ob. num.	378	384	383	386	390	388	385	382	380	380	379	377	

Table 5.1.1-16 Root mean square of vector wind errors at 250 hPa against observations (m/s)

Southern Hemisphere (20–90˚S)

Hours	Jan	Feb	Mar	Apr	May	Jun	Jul	Aug	Sep	Oct	Nov	Dec	Annual
24	5.2	5.3	5.5	5.5	5.5	5.5	5.4	5.5	5.4	5.8	5.9	5.8	5.5
72	8.0	7.9	8.9	9.0	8.9	8.5	9.4	8.7	8.5	9.1	9.0	8.6	8.7
120	11.7	11.3	12.6	13.9	14.0	13.3	14.2	12.4	12.7	13.8	13.3	12.5	13.0
ob. num.	45	43	40	39	35	36	37	40	40	42	44	45	

Table 5.1.1-17 Root mean square of vector wind errors at 850 hPa against analysis (m/s)

Tropic

Hours	Jan	Feb	Mar	Apr	May	Jun	Jul	Aug	Sep	Oct	Nov	Dec	Annual
24	1.6	1.6	1.5	1.4	1.5	1.5	1.5	1.6	1.6	1.6	1.6	1.5	1.5
72	2.7	2.7	2.5	2.5	2.6	2.6	2.7	2.8	2.8	2.8	2.7	2.7	2.7
120	3.3	3.4	3.1	3.1	3.2	3.2	3.3	3.4	3.4	3.6	3.3	3.4	3.3

Table 5.1.1-18 Root mean square of vector wind errors at 250 hPa against analysis (m/s)

Tropic

Hours	Jan	Feb	Mar	Apr	May	Jun	Jul	Aug	Sep	Oct	Nov	Dec	Annual
24	3.4	3.3	3.1	2.9	3.1	3.1	3.2	3.3	3.1	3.1	3.1	3.2	3.2
72	6.0	5.8	5.4	5.3	5.5	5.4	5.5	5.7	5.4	5.6	5.5	5.7	5.6
120	7.9	7.6	7.0	6.9	7.2	6.9	6.9	7.1	6.9	7.3	7.3	7.5	7.2

Table 5.1.1-19 Root mean square of vector wind errors at 850 hPa against observations (m/s)

Tropic

Hours	Jan	Feb	Mar	Apr	May	Jun	Jul	Aug	Sep	Oct	Nov	Dec	Annual
24	3.4	3.5	3.3	3.2	3.3	3.4	3.3	3.5	3.5	3.6	3.5	3.4	3.4
72	4.0	3.9	3.7	3.6	3.8	3.8	3.9	4.0	4.0	4.4	4.3	4.1	4.0
120	4.4	4.3	4.1	4.0	4.2	4.1	4.4	4.6	4.4	5.2	4.7	4.5	4.4
ob. num.	69	72	72	73	67	61	64	67	64	69	76	78	

Table 5.1.1-20 Root mean square of vector wind errors at 250 hPa against observations (m/s)

Tropic

Hours	Jan	Feb	Mar	Apr	May	Jun	Jul	Aug	Sep	Oct	Nov	Dec	Annual
24	4.8	4.8	4.6	4.3	4.9	4.8	4.7	4.9	4.6	4.9	4.7	4.9	4.7
72	6.3	6.4	6.0	5.7	6.6	6.4	6.5	6.9	6.2	6.7	6.1	6.4	6.4
120	7.9	7.4	6.9	6.7	7.9	7.8	7.7	8.1	7.5	8.0	7.2	7.8	7.6
ob. num.	71	73	72	75	66	56	60	63	61	68	77	80	

The Global EPS is verified against analysis values in line with the Manual on GDPFS (WMO-No. 485). The Brier Skill Score (BSS) for seasonal (DJF: December-January-February; MAM: March-April-May; JJA: June-July-August; SON: September-October-November) and annual averages in

2020(December in 2019) are shown in Tables 5.1.1-21 – 5.1.1-26.

Table 5.1.1-21 BSS for geopotential height at 500 hPa over the Northern Hemisphere (20–90°N)

Hour	Z500 anomaly +1.0 standard deviation					Z500 anomaly +1.5 standard deviation					Z500 anomaly +2.0 standard deviation				
	DJF	MAM	JJA	SON	Annual	DJF	MAM	JJA	SON	Annual	DJF	MAM	JJA	SON	Annual
24	0.924	0.926	0.889	0.915	0.914	0.903	0.918	0.866	0.895	0.896	0.855	0.906	0.825	0.855	0.861
72	0.792	0.810	0.743	0.783	0.782	0.749	0.792	0.707	0.741	0.747	0.658	0.771	0.636	0.672	0.684
120	0.628	0.646	0.557	0.606	0.609	0.582	0.623	0.511	0.543	0.565	0.473	0.575	0.419	0.453	0.480
168	0.447	0.472	0.360	0.399	0.420	0.404	0.445	0.323	0.329	0.375	0.255	0.382	0.250	0.254	0.285
Hour	Z500 anomaly -1.0 standard deviation					Z500 anomaly -1.5 standard deviation					Z500 anomaly -2.0 standard deviation				
	DJF	MAM	JJA	SON	Annual	DJF	MAM	JJA	SON	Annual	DJF	MAM	JJA	SON	Annual
24	0.899	0.913	0.867	0.904	0.896	0.871	0.896	0.844	0.880	0.873	0.842	0.882	0.799	0.841	0.841
72	0.733	0.755	0.655	0.742	0.721	0.671	0.705	0.593	0.686	0.664	0.608	0.655	0.497	0.613	0.593
120	0.518	0.543	0.413	0.537	0.503	0.428	0.471	0.328	0.450	0.419	0.354	0.398	0.230	0.363	0.336
168	0.298	0.347	0.223	0.330	0.300	0.195	0.274	0.146	0.241	0.214	0.135	0.203	0.083	0.160	0.145

Table 5.1.1-22 BSS for temperature at 850 hPa over the Northern Hemisphere (20–90°N)

Hour	T850 anomaly +1.0 standard deviation					T850 anomaly +1.5 standard deviation					T850 anomaly +2.0 standard deviation				
	DJF	MAM	JJA	SON	Annual	DJF	MAM	JJA	SON	Annual	DJF	MAM	JJA	SON	Annual
24	0.831	0.834	0.777	0.822	0.816	0.791	0.808	0.752	0.786	0.784	0.756	0.786	0.714	0.736	0.748
72	0.663	0.668	0.580	0.648	0.640	0.600	0.621	0.536	0.596	0.588	0.536	0.573	0.470	0.509	0.522
120	0.499	0.507	0.403	0.488	0.474	0.424	0.452	0.349	0.423	0.412	0.349	0.386	0.286	0.335	0.339
168	0.339	0.348	0.241	0.323	0.313	0.268	0.295	0.190	0.261	0.254	0.184	0.236	0.131	0.184	0.184
Hour	T850 anomaly -1.0 standard deviation					T850 anomaly -1.5 standard deviation					T850 anomaly -2.0 standard deviation				
	DJF	MAM	JJA	SON	Annual	DJF	MAM	JJA	SON	Annual	DJF	MAM	JJA	SON	Annual
24	0.820	0.834	0.766	0.820	0.810	0.765	0.798	0.700	0.771	0.759	0.716	0.738	0.630	0.711	0.698
72	0.664	0.668	0.546	0.657	0.634	0.602	0.609	0.448	0.597	0.564	0.533	0.522	0.361	0.544	0.490
120	0.487	0.493	0.346	0.501	0.457	0.418	0.426	0.253	0.443	0.385	0.355	0.333	0.180	0.385	0.313
168	0.300	0.307	0.188	0.343	0.284	0.222	0.246	0.111	0.285	0.216	0.156	0.151	0.064	0.228	0.150

Table 5.1.1-23 BSS for geopotential height at 500 hPa over the Tropics (20°S–20°N)

Hour	Z500 anomaly +1.0 standard deviation					Z500 anomaly +1.5 standard deviation					Z500 anomaly +2.0 standard deviation				
	DJF	MAM	JJA	SON	Annual	DJF	MAM	JJA	SON	Annual	DJF	MAM	JJA	SON	Annual
24	0.801	0.798	0.725	0.726	0.763	0.765	0.782	0.708	0.671	0.731	0.697	0.745	0.616	0.549	0.652
72	0.621	0.620	0.564	0.532	0.584	0.578	0.599	0.563	0.516	0.564	0.537	0.549	0.485	0.462	0.508
120	0.484	0.479	0.471	0.415	0.462	0.441	0.459	0.448	0.409	0.439	0.379	0.437	0.379	0.362	0.389

168	0.309	0.331	0.331	0.233	0.301	0.280	0.300	0.311	0.239	0.282	0.223	0.267	0.248	0.204	0.235
Hour	Z500 anomaly -1.0 standard deviation					Z500 anomaly -1.5 standard deviation					Z500 anomaly -2.0 standard deviation				
	DJF	MAM	JJA	SON	Annual	DJF	MAM	JJA	SON	Annual	DJF	MAM	JJA	SON	Annual
24	0.775	0.774	0.656	0.704	0.727	0.756	0.772	0.594	0.679	0.700	0.746	0.746	0.566	0.649	0.677
72	0.560	0.552	0.272	0.445	0.457	0.530	0.528	0.093	0.424	0.394	0.480	0.485	0.070	0.369	0.351
120	0.403	0.384	0.089	0.233	0.277	0.365	0.354	-0.089	0.259	0.222	0.318	0.308	-0.026	0.198	0.199
168	0.218	0.189	-0.056	0.019	0.092	0.162	0.141	-0.162	0.092	0.058	0.117	0.130	-0.133	0.077	0.048

Table 5.1.1-24 BSS for temperature at 850 hPa over the Tropics (20˚S–20˚N)

Hour	T850 anomaly +1.0 standard deviation					T850 anomaly +1.5 standard deviation					T850 anomaly +2.0 standard deviation				
	DJF	MAM	JJA	SON	Annual	DJF	MAM	JJA	SON	Annual	DJF	MAM	JJA	SON	Annual
24	0.544	0.575	0.557	0.556	0.558	0.464	0.516	0.516	0.511	0.502	0.395	0.443	0.440	0.435	0.429
72	0.274	0.317	0.352	0.330	0.318	0.197	0.258	0.317	0.312	0.271	0.159	0.214	0.247	0.263	0.221
120	0.170	0.197	0.266	0.234	0.217	0.117	0.154	0.242	0.233	0.186	0.102	0.131	0.178	0.196	0.152
168	0.091	0.119	0.201	0.161	0.143	0.060	0.086	0.188	0.174	0.127	0.065	0.087	0.134	0.145	0.108
Hour	T850 anomaly -1.0 standard deviation					T850 anomaly -1.5 standard deviation					T850 anomaly -2.0 standard deviation				
	DJF	MAM	JJA	SON	Annual	DJF	MAM	JJA	SON	Annual	DJF	MAM	JJA	SON	Annual
24	0.627	0.601	0.560	0.597	0.596	0.600	0.536	0.482	0.523	0.535	0.591	0.468	0.430	0.441	0.482
72	0.410	0.383	0.370	0.397	0.390	0.384	0.320	0.300	0.310	0.328	0.355	0.264	0.261	0.236	0.279
120	0.282	0.267	0.267	0.311	0.282	0.250	0.206	0.200	0.227	0.221	0.219	0.142	0.169	0.162	0.173
168	0.201	0.181	0.207	0.256	0.211	0.174	0.122	0.148	0.183	0.157	0.134	0.065	0.120	0.130	0.112

Table 5.1.1-25 BSS for geopotential height at 500 hPa over the Southern Hemisphere (20–90˚S)

Hour	Z500 anomaly +1.0 standard deviation					Z500 anomaly +1.5 standard deviation					Z500 anomaly +2.0 standard deviation				
	DJF	MAM	JJA	SON	Annual	DJF	MAM	JJA	SON	Annual	DJF	MAM	JJA	SON	Annual
24	0.906	0.914	0.927	0.922	0.917	0.890	0.895	0.909	0.897	0.898	0.869	0.846	0.864	0.872	0.863
72	0.763	0.765	0.790	0.789	0.777	0.739	0.727	0.741	0.741	0.737	0.710	0.645	0.655	0.701	0.678
120	0.574	0.566	0.619	0.609	0.592	0.544	0.527	0.543	0.538	0.538	0.493	0.420	0.397	0.461	0.443
168	0.380	0.354	0.431	0.415	0.395	0.334	0.303	0.350	0.346	0.333	0.285	0.218	0.210	0.245	0.239
Hour	Z500 anomaly -1.0 standard deviation					Z500 anomaly -1.5 standard deviation					Z500 anomaly -2.0 standard deviation				
	DJF	MAM	JJA	SON	Annual	DJF	MAM	JJA	SON	Annual	DJF	MAM	JJA	SON	Annual
24	0.903	0.909	0.915	0.910	0.909	0.891	0.890	0.895	0.888	0.891	0.880	0.873	0.866	0.865	0.871
72	0.739	0.730	0.749	0.743	0.740	0.712	0.683	0.697	0.694	0.697	0.676	0.639	0.632	0.642	0.647
120	0.527	0.518	0.543	0.533	0.530	0.484	0.448	0.466	0.465	0.466	0.433	0.381	0.386	0.380	0.395
168	0.338	0.305	0.352	0.330	0.331	0.300	0.245	0.284	0.260	0.272	0.259	0.176	0.201	0.179	0.204

Table 5.1.1-26 BSS for temperature at 850 hPa over the Southern Hemisphere (20–90°S)

Hour	T850 anomaly +1.0 standard deviation					T850 anomaly +1.5 standard deviation					T850 anomaly +2.0 standard deviation				
	DJF	MAM	JJA	SON	Annual	DJF	MAM	JJA	SON	Annual	DJF	MAM	JJA	SON	Annual
24	0.804	0.811	0.823	0.837	0.819	0.776	0.776	0.779	0.806	0.784	0.765	0.739	0.733	0.770	0.752
72	0.605	0.607	0.637	0.657	0.626	0.565	0.562	0.568	0.612	0.577	0.539	0.504	0.483	0.541	0.517
120	0.428	0.420	0.472	0.480	0.450	0.379	0.370	0.402	0.432	0.396	0.345	0.311	0.317	0.352	0.331
168	0.272	0.240	0.311	0.307	0.282	0.228	0.191	0.246	0.269	0.233	0.190	0.141	0.174	0.207	0.178
Hour	T850 anomaly -1.0 standard deviation					T850 anomaly -1.5 standard deviation					T850 anomaly -2.0 standard deviation				
	DJF	MAM	JJA	SON	Annual	DJF	MAM	JJA	SON	Annual	DJF	MAM	JJA	SON	Annual
24	0.800	0.823	0.837	0.842	0.826	0.780	0.786	0.789	0.813	0.792	0.766	0.723	0.712	0.758	0.740
72	0.609	0.634	0.662	0.667	0.643	0.597	0.590	0.591	0.631	0.602	0.589	0.517	0.492	0.575	0.543
120	0.432	0.442	0.478	0.487	0.460	0.426	0.397	0.387	0.442	0.413	0.416	0.340	0.287	0.386	0.357
168	0.272	0.265	0.305	0.309	0.288	0.267	0.223	0.223	0.258	0.243	0.249	0.172	0.141	0.206	0.192

5.2 Research performed in this field

6. Plans for the future (next 4 years)

6.1 Development of the GDPFS

6.1.1 Major changes expected in the next year

(1) GOES-17 AMVs and CSR data will be incorporated into the global NWP system.

(2) Bias correction for aircraft temperature in JMA's global NWP system will be improved.

(3) Total precipitable water vapor from shipborne GNSS will be incorporated into the mesoscale NWP system.

(4) Additional all-sky microwave humidity sounder radiance data will be assimilated into the global NWP system.

(5) Metop-C/AMSU-A and MHS data will be incorporated into the mesoscale and local NWP systems.

(6) Metop-C/IASI data will be incorporated into the global NWP system.

(7) The forecast model adopted in the GEPS will be replaced with the latest operational GSM.

(8) The vertical layers of the global NWP system and GEPS will be enhanced.

(9) A soil moisture analysis system will be incorporated into GA.

(10) Improvements to observation processing (such as snow cover estimation from satellite observation) will be incorporated into snow depth analysis.

(11) The number of vertical layers in the LFM will be enhanced from 58 to 76.

(12) The number of GEPS and WENS members will be increased.

(13) The number of ensemble members used to create flow-dependent background error covariances in GA and weighting for ensemble covariance will be increased.
(14) The forecast period of the Japan region storm surge model will be extended from 39 to 51 hours in April 2021. The typhoon bogus scheme in the storm surge model will be updated for better representation of surface winds in coastal areas.
(15) The results of the Japanese Reanalysis for Three Quarters of a Century (JRA-3Q) being produced with the TL479 version of JMA's operational data assimilation system as of December 2018 will be made available for the period from 1991 onward.
(16) A new atmospheric transport model for volcanic ash will be introduced with unification of the RATM and the GATM.
(17) Initial distributions for volcanic ash clouds in the atmospheric transport model will be improved with consideration for wind profile at the volcanic ash clouds.

6.1.2 Major changes expected in the next four years

(1) The horizontal resolutions of the GSM and GEPS will be improved.
(2) The physics parameterization of the global NWP system and GEPS will be upgraded.
(3) The forecast model adopted in the GEPS will be replaced with the latest operational GSM.
(4) Global snow depth analysis will be changed from one to four times a day.
(5) The physical processes of the MSM and LFM will be upgraded.
(6) The number of vertical layers in the MSM will be enhanced from 76 to 96.
(7) The MSM forecast range will be extended from 51 to 78 hours at 00 and 12 UTC initial times.
(8) Hybrid three-dimensional variational data assimilation will be incorporated into the local NWP system
(9) The number of vertical layers in the MEPS will be enhanced from 76 to 96.
(10) Mesoscale SVs based on ASUCA will be incorporated into the MEPS.
(11) Model uncertainty perturbation will be incorporated into the MEPS.
(12) The horizontal and vertical resolutions of Hourly Analysis will be enhanced, and the number of related daily operations will be increased.
(13) Metop-C/GRAS data will be incorporated into the global NWP system.
(14) Accounting for inter-channel error correlations in the assimilation of satellite radiances will be incorporated into the global NWP system.
(15) GNSS-RO bending-angle data from TanDEM-X/IGOR will be assimilated into the global NWP system
(16) The satellite radiance data used in the global NWP system (e.g., ATMS, CrIS, IASI, AIRS) will be assimilated into the mesoscale and local NWP systems.
(17) All-sky microwave radiance data will be assimilated into the mesoscale NWP system.
(18) Surface-sensitive microwave radiance data over land will be assimilated with dynamically estimated emissivity into the global NWP system.
(19) The Radiative Transfer Model used for radiance data assimilation will be updated.

(20) More satellite data, including ScatSat-1/OSCAT and VIIRS-AMV content, will be assimilated into the global, mesoscale and local NWP systems.
(21) Modification to enhance the use of aircraft data will be incorporated into the global NWP system.
(22) GPS radiosonde data on drift positions will be assimilated into the global NWP system.
(23) Observation from descending radiosonde data will be assimilated into the mesoscale NWP system.
(24) Relative humidity from AMeDAS will be assimilated into the local NWP system.
(25) Modification to enhance the use of land surface observations on a temporal scale will be incorporated into the global NWP system.
(26) Metop-C/ASCAT wind data will be incorporated into the mesoscale NWP system.
(27) The Spectral Latent Heating (SLH) product will be assimilated into the local NWP system.
(28) The 2D-Var data assimilation system will be adopted in stratospheric ozone analysis.
(29) The regional chemical transport model run frequency will be increased from once to three times a day.
(30) The vertical resolution of the chemical transport model in the UV prediction system will be enhanced from 64 to 80 or more levels.
(31) The grid resolution of the Global Wave Model (GWM) will be enhanced from 55 to 25 km.
(32) A new wave model with a 1-minute grid resolution for coastal sea areas of Japan will be put into operation.
(33) The forecast period for both storm surge models will be extended to 78 hours for the Japan region and from 72 to 132 hours for the Asian region.
(34) A new storm surge model involving the use of an unstructured grid will be incorporated, and grid resolution will be enhanced in both storm surge models.
(35) Storm surge EPSs will be incorporated into both storm surge models.
(36) An incremental 4DVAR method will be adopted for the global ocean data assimilation system (MOVE/MRI.COM) with resolution increased to 0.25 × 0.25°.
(37) The representation of physical processes and the model resolution for the Seasonal EPS will be improved.
(38) The results of the JRA-3Q re-analysis will be made available for the whole period from the late 1940s onward.

6.2 Planned research Activities in NWP, Nowcasting, Long-range Forecasting and Specialized Numerical Predictions

6.2.1 Planned Research Activities in NWP

6.2.2 Planned Research Activities in Nowcasting

(1) Use of dual polarized radar data for R/A, VSRF, Thunder Nowcasts and Hazardous Wind Potential Nowcasts

6.2.3 Planned Research Activities in Long-range Forecasting

6.2.4 Planned Research Activities in Specialized Numerical Predictions

(1) Time-of-arrival products for nuclear environmental emergency response

In line with a development plan set by the WMO/INFCOM Expert Team on Emergency Response Activities (ET-ERA), JMA is currently researching time-of-arrival products.

(2) Probability forecasts for volcanic ash

JMA is currently exploring methods to meet the needs of probability forecasts for volcanic ash as described in the International Airways Volcano Watch (IAVW) roadmap.

7. References

Aoki, Te., Ta. Aoki, M. Fukabori, and T. Takao, 2002: Characteristics of UV-B Irradiance at Syowa Station, Antarctica: Analyses of the Measurements and Comparison with Numerical Simulations. *J. Meteor. Soc. Japan.*, **80**, 161–170.

Aranami, K., T. Hara, Y. Ikuta, K. Kawano, K. Matsubayashi, H. Kusabiraki, T. Ito, T. Egawa, K. Yamashita, Y. Ota, Y. Ishikawa, T. Fujita, and J. Ishida, 2015: A new operational regional model for convection-permitting numerical weather prediction at JMA. *CAS/JSC WGNE Res. Activ. Atmos. Oceanic Modell.*, **45**, 5.05-5.06.

Buizza, R., and T. N. Palmer, 1995: The singular-vector structure of the atmospheric global circulation. *J. Atmos. Sci.*, **52**, 1434–1456.

Deushi, M., and K. Shibata, 2011: Development of an MRI Chemistry-Climate Model ver. 2 for the study of tropospheric and stratospheric chemistry, *Papers in Meteorology and Geophysics,* **62**, 1 – 46.

Egbert, G., and S. Erofeeva, 2002: Efficient Inverse Modeling of Barotropic Ocean Tides. *J. Atmos. Oceanic Technol.*, **19**, 183–204.

Ehrendorfer, M., R. M. Errico, and K. D. Raeder, 1999: Singular-Vector Perturbation Growth in a Primitive Equation Model with Moist Physics. *J. Atmos. Sci.*, **56**, 1627–1648.

Foster, D. J., and R. D. Davy, 1988: *Global Snow Depth Climatology.* USAF-ETAC/TN-88/006. Scott Air Force Base, Illinois, p. 48.

Hasegawa, Y., A. Sugai, Yo. Hayashi, Yu. Hayashi, S. Saito, and T. Shimbori, 2015: Improvements of volcanic ash fall forecasts issued by the Japan Meteorological Agency. *J. Appl. Volcanol.*, **4**: 2.

Hamrud, M., M. Bonavita, and L. Isaksen, 2015: EnKF and hybrid gain ensemble data assimilation. Part I: EnKF implementation. *Mon. Wea. Rev.*, **143**, 4847–4864.

Hirose, N., N. Usui, K. Sakamoto, H. Tsujino, G. Yamanaka, H. Nakano, S. Urakawa, T. Toyoda, Y. Fujii, and N. Kohno 2019: Development of a new operational system for monitoring and forecasting coastal and open-ocean states around Japan. *Ocean Dynamics*, **69(11)**, 1333-1357.

Honda, Y., M. Nishijima, K. Koizumi, Y. Ohta, K. Tamiya, T. Kawabata, and T. Tsuyuki, 2005: A pre-operational variational data assimilation system for a non-hydrostatic model at the Japan Meteorological Agency: Formulation and preliminary results. *Quart. J. Roy. Meteor. Soc.*, **131**, 3465-3475.

Hunt, B. R., E. J. Kostelich, and I. Szunyogh, 2007: Efficient data assimilation for spatiotemporal chaos: A local ensemble transform Kalman filter. *Physica D*, **230**, 112–126.

Ikuta, Y., H. Kusabiraki, K. Kawano, T. Anzai, M. Sawada, M. Ujiie, S. Nishimoto, Y. Ota, and M. Narita, 2020: A New Data Assimilation System and Upgrading of Physical Processes in JMA's Meso-scale NWP System. *CAS/JSC WGNE Res. Activ. Atmos. Oceanic Modell.*, **50**, 1.07–1.08.

Ishida, J., C. Muroi, and Y. Aikawa, 2009: Development of a new dynamical core for the nonhydrostatic model. *CAS/JSC WGNE Res. Activ. Atmos. Oceanic Modell.*, **39**, 05.09–05.10.

Ishida, J., C. Muroi, K. Kawano, and Y. Kitamura, 2010: Development of a new nonhydrostatic model "ASUCA" at JMA. *CAS/JSC WGNE Res. Activ. Atmos. Oceanic Modell.*, **40**, 05.11–05.12.

Ishikawa, Y., and K. Koizumi, 2002: Meso-scale analysis. *In Outline of the Operational Numerical Weather Prediction at the Japan Meteorological Agency. Appendix to WMO Technical Progress Report on the Global Data-processing and Forecasting Systems (GDPFS) and Numerical Weather Prediction (NWP) Research*. Japan Meteorological Agency, Tokyo, Japan, 26–31. (https://warp.da.ndl.go.jp/info:ndljp/pid/246209/www.jma.go.jp/jma/jma-eng/jma-center/nwp/outline-nwp/index.htm)

JMA., 2019: Computer System, *In Outline of the Operational Numerical Weather Prediction at the Japan Meteorological Agency. Appendix to WMO Technical Progress Report on the Global Data-processing and Forecasting Systems (GDPFS) and Numerical Weather Prediction (NWP) Research.* Japan Meteorological Agency, Tokyo, Japan, 1–7. (https://www.jma.go.jp/jma/jma-eng/jma-center/nwp/outline2019-nwp/index.htm)

Kajino, M., M. Deushi, T. T. Sekiyama, N. Oshima, K. Yumimoto, T. Y. Tanaka, J. Ching, A. Hashimoto, T. Yamamoto, M. Ikegami, A. Kamada, M. Miyashita, Y. Inomata, S. Shima, A. Takami, A. Shimizu, S. Hatakeyama, Y. Sadanaga, H. Irie, K. Adachi, Y. Zaizen, Y. Igarashi, H. Ueda, T. Maki, and M. Mikami, 2019: NHM-Chem, the Japan Meteorological Agency's regional meteorology – chemistry model: model evaluations toward the consistent predictions of the chemical, physical, and optical properties of aerosols, *J. Meteor. Soc. Japan*, **97(2)**, 337-374.

Kajino, M., N. Tanji, and M. Kuramochi, 2021: Better prediction of surface ozone by a superensemble method using emission sensitivity runs in Japan, *Atmos. Environ.* X, in review.

Kakehata, K., M. Kunii, K. Kawano, and H. Kawano, 2021: Upgrade of JMA's Mesoscale Ensemble Prediction System. *CAS/JSC WGNE Res. Activ. Atmos. Oceanic Modell.,* **51**, 5.05–5.06.

Kikuchi, M., H. Murakami, K. Suzuki, T. M. Nagao, and A. Higurashi, 2018: Improved Hourly Estimates of Aerosol Optical Thickness Using Spatiotemporal Variability Derived From Himawari-8 Geostationary Satellite. *IEEE Transactions on Geoscience and Remote Sensing,*

56(6), 3442-3455, doi:10.1109/TGRS.2018.2800060.

Kobayashi, S., Y. Ota, Y. Harada, A. Ebita, M. Moriya, H. Onoda, K. Onogi, H. Kamahori, C. Kobayashi, H. Endo, K. Miyaoka, and K. Takahashi, 2015: The JRA-55 reanalysis: General specifications and basic characteristics. *J. Meteor. Soc. Japan*, **93**, 5-48.

Kohno, N., D. Miura, and K. Yoshita, 2012: The Development of JMA Wave Data Assimilation System. Proceeding of 12th International Workshop on Wave Hindcasting and Forecasting & 3rd Coastal Hazard Symposium, H2.
(https://www.waveworkshop.org/12thWaves/papers/full_paper_Kohno_et_al.pdf)

Koren, B., 1993: A Robust Upwind Discretization Method For Advection, Diffusion And Source Terms. *CWI Technical Report NM-R* **9308**, 1-22.

Kurihara, Y., H. Murakami, and M. Kachi, 2016: Sea surface temperature from the new Japanese geostationary meteorological Himawari-8 satellite, *Geophysical Research Letters*, **43(3)**, 1234-40.

Lorenc, A. C., 2003. The potential of the ensemble Kalman filter for NWP: a comparison with 4D-Var. Quart. *J. Roy. Meteor. Soc.*, **129**, 3183 – 3203.

Okabe, I., 2019a: Operational use of surface-sensitive clear-sky radiance data in JMA's mesoscale NWP system. *CAS/JSC WGNE Research Activities in Atmospheric and Oceanic Modelling, Rep.* **49**, 1-15.

Okabe, I., 2019b: Operational use of surface-sensitive clear-sky radiance data in JMA's global NWP system. *CAS/JSC WGNE Research Activities in Atmospheric and Oceanic Modelling, Rep*. **49**, 1-17.

Okabe, I., 2021: Operational use of Himawari-8 CSR data of band 9 and 10 in JMA's local NWP system. *CAS/JSC WGNE Research Activities in Atmospheric and Oceanic Modelling, Rep.* **51**, 1-11.

Onogi, K., J. Tsutsui, H. Koide, M. Sakamoto, S. Kobayashi, H. Hatsushika, T. Matsumoto, N. Yamazaki, H. Kamahori, K. Takahashi, S. Kadokura, K. Wada, K. Kato, R. Oyama, T. Ose, N. Mannoji, and R. Taira, 2007: The JRA-25 reanalysis. *J. Meteor. Soc. Japan*, **85**, 369-432.

Ono, K., Y. Honda, and M. Kunii 2011: A mesoscale ensemble prediction system using singular vector methods. *CAS/JSC WGNE Res. Activ. Atmos. Oceanic Modell.*, **41**, 5.17-5.18.

Ono, K., 2017: Consistent Initial and Lateral Boundary Perturbations in Mesoscale Ensemble Prediction System at JMA. CAS/JSC WGNE Res. Activ. Atmos. Oceanic Modell., **47**, 5.16-5.17.

Ono, K., M. Kunii, and Y. Honda, 2021: The regional model-based Mesoscale Ensemble Prediction System, MEPS, at the Japan Meteorological Agency. *Quart. J. Roy. Meteor. Soc.*, **147**, 465–484.

Palmer, T. N., R. Buizza, F. Doblas-Reyes, T. Jung, M. Leutbecher, G. J. Shutts, M. Steinheimer, and A. Weisheimer, 2009: Stochastic parametrization and model uncertainty. *ECMWF Technical Memoranda*, **598**, 42pp.

Saito, K., T. Fujita, Y. Yamada, J. Ishida, Y. Kumagai, K. Aranami, S. Ohmori, R. Nagasawa, S. Kumagai, C. Muroi, T. Kato, H. Eito, and Y. Yamazaki, 2006: The operational JMA Nonhydrostatic Mesoscale Model. *Mon. Wea. Rev.*, **134**, 1266-1298.

Saito, K., J. Ishida, K. Aranami, T. Hara, T. Segawa, M. Narita, and Y. Honda, 2007: Nonhydrostatic

Atmospheric Models and Operational Development at JMA. *J. Meteor. Soc. Japan*, **85B**, 271-304.

Sakamoto, K., H. Tsujino, H. Nakano, S. Urakawa, T. Toyoda, N. Hirose, N. Usui, and G. Yamanaka, 2019: Development of a 2-km resolution ocean model covering the coastal seas around Japan for operational application. *Ocean Dynamics*, **69(10)**, 1181-1202.

Shimbori, T., Y. Aikawa, and N. Seino, 2009: Operational implementation of the tephra fall forecast with the JMA mesoscale tracer transport model. *CAS/JSC WGNE Res. Activ. Atmos. Oceanic Modell.*, **39**, 5.29–5.30.

Shimizu, H., M. Kazumori, and T. Kadowaki, 2020: Implementation of all-sky microwave radiance assimilation into JMA's global NWP system. *CAS/JSC WGNE Research Activities in Atmospheric and Oceanic Modelling, Rep.* **50**, 1-21.

Takakura, T., and T. Komori, 2020: Two-tiered sea surface temperature approach implemented to JMA's Global Ensemble Prediction System. *WGNE. Res. Activ. Earth System. Modell.,* **50**, 6.15-6.16.

Takano, I., Y. Aikawa, and S. Gotoh, 2007: Improvement of photochemical oxidant information by applying transport model to oxidant forecast. *CAS/JSC. WGNE. Res. Activ. Atmos. Oceanic Modell.*, **37**, 5.35–5.36.

Tanaka, T. Y., and M. Chiba, 2005: Global simulation of dust aerosol with a chemical transport model, MASINGAR. *J. Meteor. Soc. Japan*, **83A**, 255–278.

Toyoda, T., Y. Fujii, T. Yasuda, N. Usui, T. Iwao, T., Kuragano, and M. Kamachi, 2013: Improved analysis of seasonal-interannual fields using a global ocean data assimilation system. *Theoretical and Applied Mechanics Japan*, **61**, 31-48

Ujiie, M., M. Higuchi, T. Kadowaki, Y. Kuroki, K. Miyaoka, M. Oda, K. Ochi, R. Sekiguchi, H. Shimizu, S. Yokota, and H. Yonehara, 2021: Upgrade of JMA's Operational Global NWP system. *WGNE Res. Activ. Earth System Modell.,* **51**, 6.09-6.10.

Yamaguchi, H., M. Ikegami, T. Iwahira, K. Ochi, R. Sekiguchi, and T. Takakura, 2021: Upgrade of JMA's Global Ensemble Prediction System. *WGNE Res. Activ. Earth System Modell.*, **51**, 6.13-6.14.

Yokota, S., T. Kadowaki, M. Oda, and Y. Ota, 2021: Improving ensemble-based background error covariances of the hybrid 4DVar in JMA's global analysis. *WGNE Res. Activ. Earth System Modell.*, **51**, 1.27-1.28.

Yoshida, M., M. Kikuchi, T. M. Nagao, H. Murakami, T. Nomaki, and A. Higurashi, 2018: Common Retrieval of Aerosol Properties for Imaging Satellite Sensors. *Journal of the Meteorological Society of Japan. Ser. II*, **96B**, 193-209. doi:10.2151/jmsj.2018-039

Yoshida, M., K. Yumimoto, T. M. Nagao, T. Y. Tanaka, M. Kikuchi, and H. Murakami, H., 2021: Satellite retrieval of aerosol combined with assimilated forecast, *Atmos. Chem. Phys.*, **21**, 1797–1813, https://doi.org/10.5194/acp-21-1797-2021

Yoshimura, H., and S. Yukimoto, 2008: Development of a Simple Coupler (Scup) for Earth System Modeling, *Papers in Meteorology and Geophysics*, **59**, 19-29.

Yukimoto, S., H. Yoshimura, M. Hosaka, T. Sakami, H. Tsujino, M. Hirabara, T. Y. Tanaka, M. Deushi,

A. Obata, H. Nakano, Y. Adachi, E. Shindo, S. Yabu, T. Ose, and A. Kitoh, 2011: Meteorological Research Institute-Earth System Model Version 1 (MRI-ESM1) - Model Description -, *Technical Reports of the Meteorological Research Institute*, **64**, ISSN 0386-4049, Meteorological Research Institute, Japan.

Yukimoto, S., Y. Adachi, M. Hosaka, T. Sakami, H. Yoshimura, M. Hirabara, T. Y. Tanaka, E. Shindo, H. Tsujino, M. Deushi, R. Mizuta, S. Yabu, A. Obata, H. Nakano, T. Koshiro, T. Ose, and A. Kitoh, 2012: A New Global Climate Model of the Meteorological Research Institute: MRI-CGCM3 —Model Description and Basic Performance—. *J. Meteor. Soc. Japan*, **90A**, 23-64, doi:10.2151/jmsj.2012-A02.

Yumimoto, K., T. Y. Tanaka, N. Oshima, and T. Maki, 2017: JRAero: the Japanese Reanalysis for Aerosol v1.0, *Geosci. Model Dev.*, **10**, 3225-3253, doi:10.5194/gmd-10-3225-2017.